


Review

# Metal–Organic Frameworks (MOFs) and Covalent Organic Frameworks (COFs) Applied to Photocatalytic Organic Transformations

Alberto López-Magano <sup>1</sup>, Alicia Jiménez-Almarza <sup>1</sup>, Jose Alemán <sup>2,3,\*</sup> and Rubén Mas-Ballesté <sup>1,3,\*</sup>

<sup>1</sup> Inorganic Chemistry Department, Módulo 7, Facultad de Ciencias, Universidad Autónoma de Madrid, 28049 Madrid, Spain; alberto.lopezmagano@uam.es (A.L.-M.); alicia.jimenez@uam.es (A.J.-A.)

<sup>2</sup> Organic Chemistry Department, Módulo 1, Facultad de Ciencias, Universidad Autónoma de Madrid, 28049 Madrid, Spain

<sup>3</sup> Institute for Advanced Research in Chemical Sciences (IAdChem), Universidad Autónoma de Madrid, 28049 Madrid, Spain

\* Correspondence: jose.aleman@uam.es (J.A.); ruben.mas@uam.es (R.M.-B.)

Received: 15 June 2020; Accepted: 24 June 2020; Published: 27 June 2020



**Abstract:** Among the different alternatives for catalysis using metal–organic frameworks (MOFs) or covalent organic frameworks (COFs), photocatalysis has remarkably evolved during the last decade. Photocatalytic reticular materials allowed recyclability and easy separation of catalyst from the product, also reaching the activity and selectivity commonly observed for molecular systems. Recently, photocatalytic MOFs and COFs have been applied to synthetic applications in order to obtain organic molecules of different complexity. However, although a good number of works have been devoted to this issue, an updated comprehensive revision on this field is still needed. The aim of this review was to fill this gap covering the following three general aspects: (1) common strategies on the design of reticular photocatalytic materials, (2) a comprehensive discussion of the photocatalytic organic reactions achieved by the use of COFs and MOFs, and (3) some critical considerations highlighting directions that should be considered in order to make advances in the study of photocatalytic COFs and MOFs.

**Keywords:** photocatalysis; metal–organic frameworks; MOF; covalent organic frameworks; COF

## 1. Introduction

Chemistry has classically addressed questions related to how atoms are linked into molecules and how molecules interact and/or react with each other. Thus, remarkable achievements have been done in the study of molecules and polymers, but extended 2D and 3D structures remained underexplored until the beginning of this century. In order to fill this gap, over the last 20 years, a large effort has been devoted to applying concepts learned at the molecular level to the design of 2D and 3D materials. First, linkage of organic molecules and metal ions resulted in the formation of metal–organic frameworks (MOFs) [1]. Later, condensation of organic molecules allowed the isolation of covalent organic frameworks (COFs) [2]. Therefore, these developments offered an unprecedented research playground that can be described as the “chemistry beyond the molecule” and is nowadays known as reticular chemistry [3].

The opportunities that reticular chemistry offers are related to the following common features in this family of materials: (a) predesign of building blocks enables control over the frameworks geometries and chemical properties; (b) structural, thermal, and chemical stabilities can be tuned by modulating the strength of bonds that result in the propagation of frameworks, and (c) crystallinity makes possible

the ultimate structural characterization by diffraction techniques. Taken together, the application of these concepts resulted in an extensive structural control and an exceptional library of protocols intended to direct the physical and/or chemical properties that can be used in many applications of frameworks. Following these principles, over the last two decades, more than eighty thousand MOFs and hundreds of COFs have been described. The fastest growing of the field of MOFs can be, in part, due to the fact that crystallinity is more easily achieved from MOFs (generally characterized from single crystal techniques) than for COFs which are usually presented as microcrystalline samples.

In general, coordination preferences of metal ions determine the geometry of metallic clusters into the MOFs. Furthermore, the multi-dentate organic ligands can control the direction of metal ions to a specific geometry and coordination. However, some centers with  $d^0$  (such as  $Zr^{IV}$ ) and  $d^{10}$  (e.g.,  $Zn^{II}$ ) electron configuration possess many coordination possibilities making more challenging the control over the structure of many MOFs. Rigid and directional polynuclear clusters known as Secondary building units (SBUs, which are polymetallic fragments that act as nodes among the organic building blocks) lock metal ions in a coordinating position and geometry into the MOFs structures. Secondary building units with the organic linkers control the geometry, allowing different structures and ensuring stability and porosity which can be modified by the link, size, length, and even functional groups. In addition to the previous design, these structures can also be post-synthetically transformed to achieve different properties and to render several applications. The distinct behavior of metal ions and clusters as well as of different organic compounds incorporated into the organic linker or encapsulated into the porous structure, constitutes an excellent opportunity to furtherly modulate and direct the MOFs' performance for different applications. It is worth noting that some interesting properties, such as structural tunability and pore size control, conductivity, high surface area, stability, and in some cases flexibility, place MOFs as appropriate materials to perform several applications, such as gas separation, cation conductivity storage, adsorption or delivery, ion-exchange, sensing or catalysis, among others [4–6].

Following a different approach, COFs are constructed by the assembly or condensation of organic building blocks through different type of covalent linkages, conferring them lower density and higher thermal and chemical stability. The geometry and length of the monomers determine the structure, dimensionality, topology, pore size, and pore shape of the framework. The corresponding building blocks are generally rigid and contain reactive groups with a predetermined symmetry. Therefore, the limitation in obtaining desired geometries of MOFs can be mitigated by the condensation of organic molecules into COFs due to the high directionality of covalent bonds, making possible the adequate combination of the molecular building units with distinct metric characteristics (i.e., size, length or angles). In principle, all the methodologies developed on the field of organic chemistry would be useful for the isolation of this class of materials. However, only the reactions that present a high degree of chemical reversibility have allowed the construction of crystalline and porous frameworks, an essential requirement to consider the mesh-material as a true COF. Thus, up to now, the most common class of covalent linkages employed in the construction of COFs are boroxine, boronate ester, imine,  $\beta$ -ketoenamine, hydrazine, and cyanovinylene bonds, among others (Figure 1) [7]. This versatility was transferred into their multiple applications, such as storage, separation or adsorption of gases, optoelectricity, sensing, drug delivery, and catalysis [7–10].

The most common topologies on COFs are hexagonal for 2D COFs and diamond-like for 3D COFs, which result from connection of linear, trigonal or tetrahedral building blocks. Interestingly, the porosity of layered COFs depends on the relative stacking of layers. Thus, for example, the stacking of COF sheets in an eclipsed manner can involve the formation of 1D channels (Figure 2) [8–11].

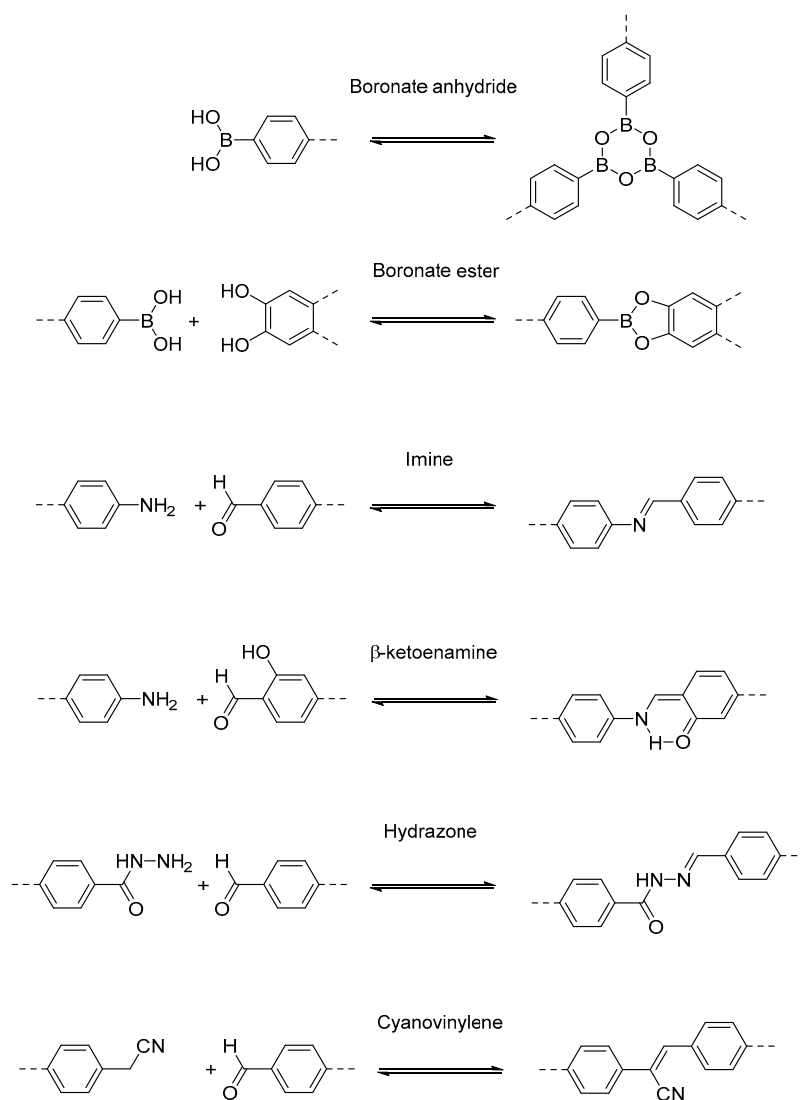


**Figure 1.** Most used type of linkages in the construction of covalent organic frameworks (COFs).

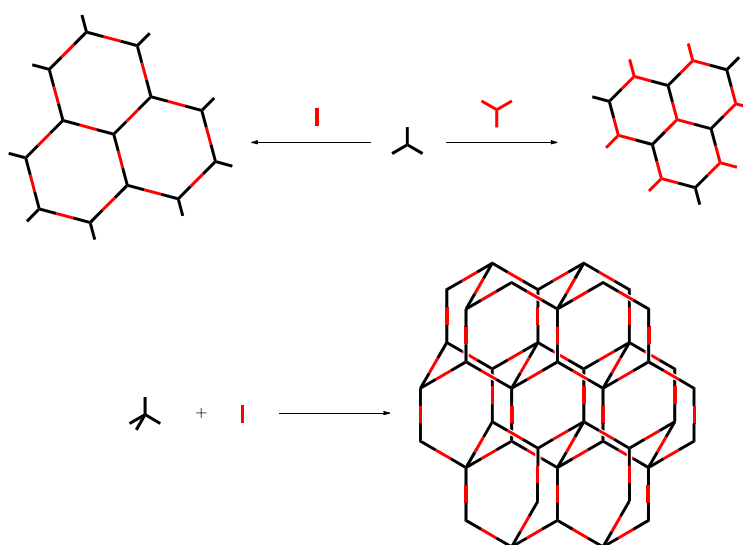


**Figure 2.** The most common topologies on layered 2D and 3D COFs.

Among the applications of reticular materials, catalysis stands out for being fundamental in organic synthesis and commonly used for obtaining a wide variety of chemical products such as pharmaceutical or agrochemical compounds. From a practical point of view, heterogeneous catalysis is always a desirable approach, because it leads to recyclability and easy separation of the catalyst from the product [11]. In fact, the activity and selectivity achieved through homogeneous catalysis are not always feasible through heterogeneous systems. In this context, reticular chemistry offers new opportunities, because it allows the incorporation of complex molecular fragments into extended porous materials. So, design of molecular catalysts can boost the development of catalytic materials based on the reticular chemistry principles that put together the best of both homogeneous and heterogeneous worlds. A particularly interesting kind of catalysis, initially developed from a molecular perspective, is photocatalysis [12–15]. In this area, photocatalysts are structures able to harvest light energy to overcome kinetic and/or thermodynamic barriers, triggering, directing and accelerating reactions in presence of light that otherwise would be prohibitive. This approach is highly interesting, because of the potential use of sunlight as a clean and free source of energy. Therefore, visible-light photocatalysis using low energy/power irradiation systems is preferable to ultraviolet photocatalysis. In addition, photocatalysis can result on obtaining products with high economic relevance such as H<sub>2</sub> production to be used as fuel, CO<sub>2</sub> revalorization or the synthesis of complex organic molecules.

In some pathways commonly observed in photocatalysis, the light is absorbed by the photocatalyst, which in the excited state becomes a powerful oxidant or reducing agent or, in some cases, both [16]. Then, electron transfer processes result in the formation of transient radical species that eventually evolve towards the desired products or otherwise are involved in undesired side reactions (Figure 3). Alternatively, the energy absorbed by the photocatalyst is directly transferred to a reagent (instead of promoting an electron transfer), resulting in its activation and then triggering the corresponding chemical process. Although the relationship between structure and photoactivity is not an obvious issue, two main requirements should be achieved: absorption of light at the appropriate wavelength and relaxation processes slower than activation of the desired reactions. A common way to reach these goals is the use of rigid highly conjugated organic structures [12]. Moieties with these characteristics can be readily incorporated into reticular materials. In particular, MOFs and COFs have allowed the inclusion of suitable  $\pi$ -units into their well-ordered extended structures that confer photocatalytic activity.

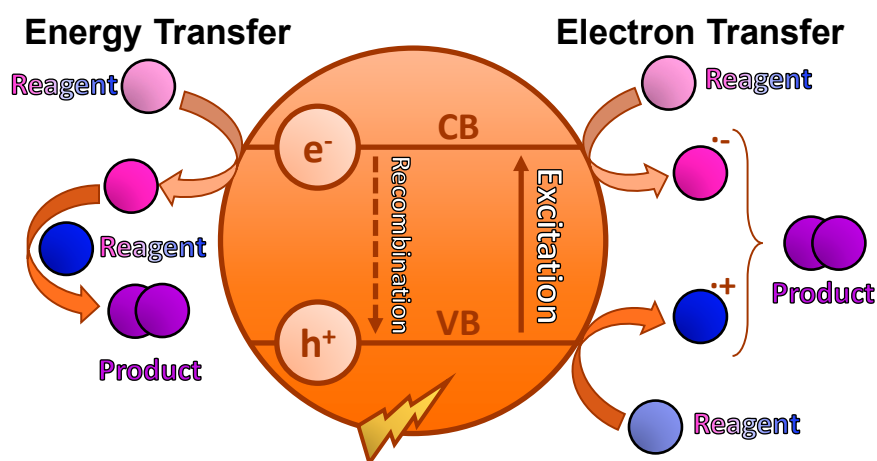


**Figure 3.** Energy transfer and electron transfer processes in photocatalysis.

From the reasons presented above, it can be inferred that MOFs and COFs represent a promising sustainable alternative to mediate photocatalytic processes. The possibility of fine tuning of their physicochemical properties through the design at the molecular level transferred to materials science open a wide range of opportunities in the design of light-harvesting antennae and photocatalytic systems. Photocatalytic applications of MOFs and COFs have been initially explored for artificial photosynthesis



and CO<sub>2</sub> reduction [17,18] or pollutant degradation processes [19]. These transformations are of undoubtable interest, owing to their environmental implications and, thus, is easy to understand why they attracted much attention during the last few years. As a consequence of this interest, some excellent reviews have been recently published overviewing the current state of the art of this field, in artificial photosynthesis and CO<sub>2</sub> reduction [18–20]. However, a more recent approach to the use of MOFs and COFs as photocatalytic materials consists of synthetic applications to achieve different organic transformations in order to obtain molecules of different complexity. Our exploration of the available literature revealed that a good number of reports have been devoted to this issue in the recent years. *In contrast, there is a lack of an updated comprehensive review addressing the application of reticular chemistry to the photocatalytic synthesis of organic compounds.* Thus, this review is intended to fill this gap presenting, first, the common strategies on the design of reticular photocatalytic materials related with their use in organic synthesis. Later, a comprehensive discussion of the reactions reported will be presented. Finally, some critical comparative considerations will be made, highlighting some factors that should be carefully taken into account on the study of such systems.

## 2. Strategies Applied on the Design of Photocatalytic MOFs and COFs

Metal–Organic Frameworks can combine the physicochemical properties of their organic and inorganic constituting parts because of their intrinsic hybrid nature. Both linkers and SBUs can act as isolated catalytic centers or, in the case of this review, as photosensitizer entities, enabling a wide range of photocatalytic organic transformations. Design of MOFs consist of the adequate combination of polytopic ligands and metal centers [1]. The most used kind of ligands are carboxylates. Typically, di- and tri-carboxylic ligands can adapt to a variety of coordination environments and materials topologies. Imidazolates are used to construct MOFs with zeolitic structures known as zeolitic imidazolate frameworks (ZIFs) [21]. Other nitrogen containing ligands, such as pyridinic compounds, are often used as pillar ligands, conferring an extra-stabilization to the 3D porous frameworks. The choice of metal center determines not only the structure but also the stability of the resulting MOF. Many metal centers have been employed in the field of MOFs, being very common the use of, for instance, zinc, zirconium, titanium, iron, and copper which are most representative of MOFs shown in this review. The different structural motifs of all the MOFs that have been employed as photocatalysts for organic reactions are represented in Figure 4.

In contrast with the straightforward strategies found for MOFs, more complex methodological issues should be considered in the design of photoactive COFs. Despite boron-containing COFs being initially reported by Yaghi et al. [2] in 2005 and representing the first successful isolation of this class of reticular materials, they did not present high stability because of their sensitivity towards the hydrolysis processes. This inconvenient has caused that photocatalytic applications of boroxine- and boronate-based COFs to remain very scarce up to now. Thus, more stable-types of linkages, most of them devoted to the formation of C–N bonds, were lately employed in the construction of photoactive COFs. Among them, imines have a leading role [22]. They are synthesized through the condensation between amines and aldehydes (which are both readily accessible) in presence of a Bronsted or Lewis acid catalyst. Although their stability towards hydrolysis is higher, the presence of strong nucleophiles is still dangerous for the maintenance of their integrity. Therefore, different strategies have been developed in order to overcome this drawback such as the oxidation into amide bonds [23] or the formation of fully conjugated COFs [24].  $\beta$ -Ketoamine-based COFs, a special type derived from imine-based COFs, are also relevant since hydroxyl groups present in the aldehyde building block facilitate the condensation reaction, and the stability of the corresponding material is increased. Moreover, in regard to the field of photochemistry, this type of linkage results are quite interesting, because the lifetime of the triplet excited state is enhanced by the presence on keto-functionalities [25]. However, the first example where a COF was employed as heterogeneous photocatalyst consisted on the photoactivated hydrogen evolution reaction (HER) mediated by a hydrazone-based COF [26]. This type of linkage, formed by the condensation between hydrazides and

aldehydes, present an increased stability towards nucleophiles, oxidants, and hydrolytic processes. In addition, hydrogen-bonding sites are accessible, since it possesses an amide-type group. Due to the insolubility and poor reactivity of the hydrazide building blocks, polar alkyl chains are often included in the structural design of such starting materials [27]. Finally, cyanovinylene-based COFs have been less explored in the field of photochemistry. They are synthesized through the Knoevenagel condensation, presenting good degrees of crystallinity, porosity, and stability. Electron delocalization is enhanced in this type of COFs, since they are totally composed by  $Csp^2-Csp^2$  bonds [28].

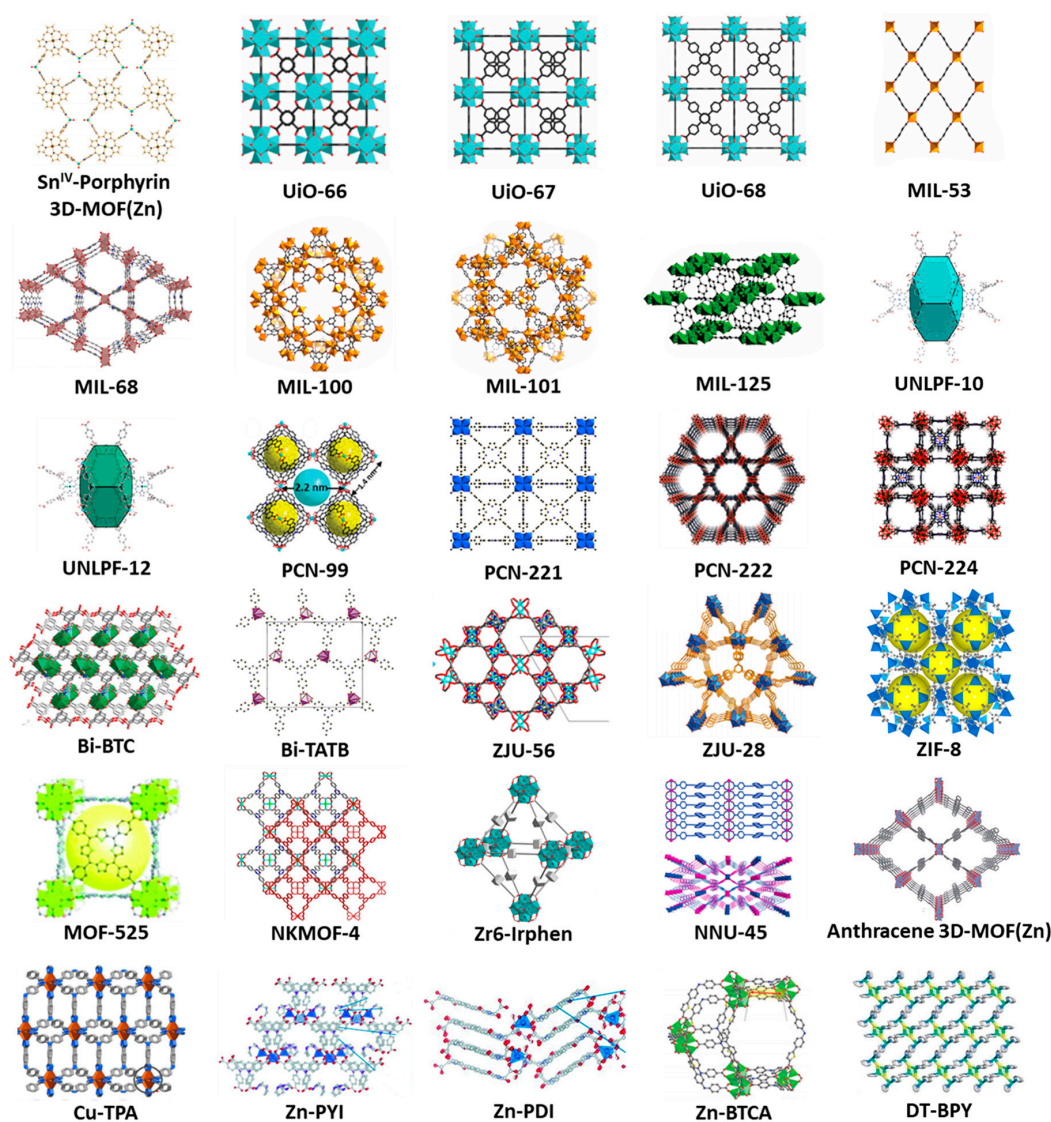
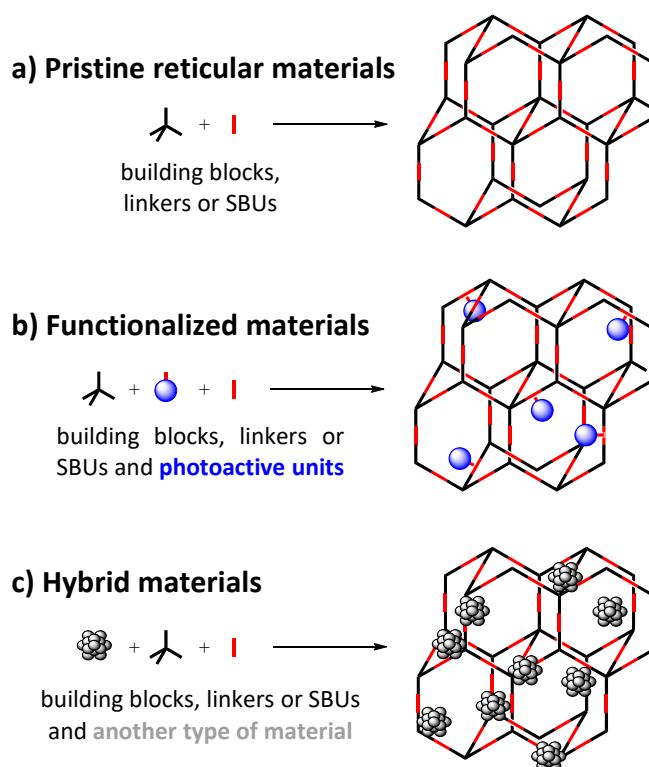


**Figure 4.** Structural motifs of MOFs applied into photocatalytic organic transformations. Adapted with permission from: Reference [29] Copyright (2011) American Chemical Society; Reference [30] Copyright (2013) American Chemical Society; Reference [31] Copyright (2014) American Chemical Society; Reference [32] Copyright (2015) American Chemical Society; References [33–36] Copyright (2019) American Chemical Society; References [37–40] with permission from John Wiley and Sons; References [41–48] with permission from The Royal Society of Chemistry; Reference [49] with permission from the Centre National de la Recherche Scientifique (CNRS) and The Royal Society of Chemistry; Reference [50] Published by the Royal Society of Chemistry; References [51,52] with permission from Elsevier.

Once these general considerations about MOFs and COFs are established, this review has categorized the following three different strategies that comprise the set of available reports devoted to the design of photocatalytically active reticular materials:

- Pristine materials:** are those MOFs or COFs composed solely by one structural backbone which does not contain attached functional molecules. The activity of these materials can be due to the intrinsic properties of the employed building blocks or can be the result of the combination of inactive building blocks that generates a photoactive framework.
- Functionalized materials:** These are the result of attached functional fragments to pristine materials. While pristine materials are not necessarily active, their functionalization incorporate photoactive moieties that remain attached to the frameworks by means of either supramolecular interactions or covalent bonding.
- Hybrid materials:** This class of structure are the result of a combination of two or more materials. Hybrid reticular materials can be the combination of various MOFs and/or COFs. Also, MOFs or COFs can be combined with carbon-based materials (graphene, carbon nitrides, etc.) or with metal nanoparticles. Such combinations usually present synergistic phenomena arising from the combination of the properties of their components.

Scheme 1 show a graphical representation of these general strategies, which are presented in detail below.



**Scheme 1.** Graphical representation of the three different strategies applied in the design of photoactive MOFs and COFs: (a) Pristine reticular materials. (b) Functionalized materials. (c) Hybrid materials.

### 2.1. Pristine Reticular Materials

First of all, the employment of pristine materials stands out for its simplicity: there is no need of functionalization protocols or incubation processes. In turn, several sub-strategies are recurrent in the design of this pristine frameworks.

On the one hand, for MOFs, the photocatalytic activity can be triggered by the SBUs or the metal nodes. In particular, the structural modification of the linker by the introduction of  $\text{-NH}_2$  groups is

quite typical, because it enables the visible-light absorption in a wide variety of MOFs and allows the transference of electrons from the linkers to the metallic clusters [47]. In other cases, for example, Fe–O or Ti<sup>IV</sup>–O clusters present intrinsic photocatalytic activity towards the formation of reactive oxygen species, which can be used in energy transfer and electron transfer reactions [53,54]. Moreover, predesign and synthesis of intrinsically photoactive linkers (such as anthracene [36], triphenylamine [52], triazine [55], porphyrin [29], tetraphenylethylene [56], perylendiimide [57], benzoselenadiazole [58], and Ir/Ru-metal complexes [59]) are also important (Figure 5).

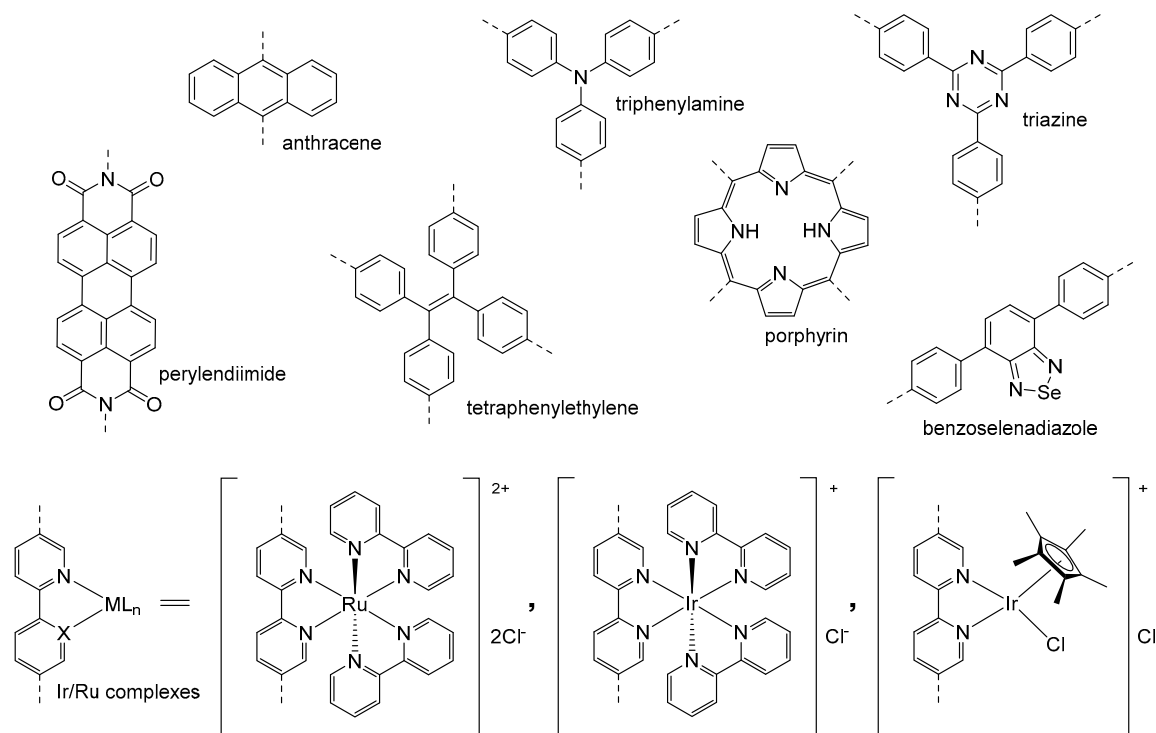


**Figure 5.** Photoactive incorporated linkers in pristine MOFs.

On the other hand, in the field of COFs, the use of pristine heterogeneous catalysts represents the most employed strategy for the design of this photocatalytically active materials. The same sub-strategies are observed in comparison with the field of MOFs. In this case, the enhanced electronic delocalization on conjugated organic frameworks has allowed the isolation of pristine materials with adequate photophysical properties for photocatalytic organic reactions.

A special type of conjugated porous organic polymers that present very similar characteristics to COFs are covalent triazine frameworks (CTFs). These polymeric materials are usually obtained from cyclotrimerization of aromatic nitriles under different specific conditions: using ionothermal synthesis, under the presence of strong acids, through Friedel–Crafts reaction or by amidine-mediated procedures [60]. They present a long-term stability and are considered as an important family of heterogeneous catalysts for industrial purposes. Although most of the reported CTFs are generally amorphous, some crystalline and porous samples have been isolated, combining the necessary conditions to be considered as COFs. Therefore, CTFs are also included in this review. In addition, the contribution of CTFs to the field of organic photochemistry is quite important. In fact, some theoretical studies predicted the behavior of pristine CTFs as organic semiconductors, which, in combination with their structural versatility allows the fine tuning of their photophysical properties. Thus, CTFs are excellent candidates to be applied on the heterogeneous photocatalysis field [61]. However, it is important to differentiate between CTFs and triazine-containing COFs. While in CTFs, the triazine unit is formed during the solvothermal treatment, using as starting materials aromatic nitriles (Figure 6, left), in triazine-containing COFs the triazine unit is pre-incorporated in

the design of one of the constituting building blocks of the material, which will be formed by the condensation through one of the linkage types explained above (Figure 6, right).

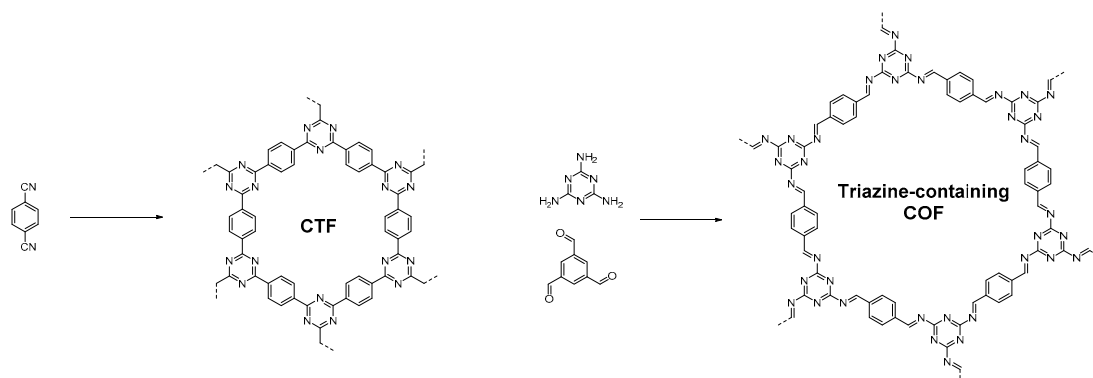


**Figure 6.** Structural differences between covalent triazine frameworks (CTFs) and triazine-containing COFs.

Other organic materials that have been proven to be useful as photocatalysts are imine- [62],  $\beta$ -ketoenamine [25], and hydrazone [27] pristine COFs [24]. This sub-strategy would be equivalent to the observed intrinsic photocatalytic activity of SBUs or metal nodes in MOFs: the resultant photoactivity is caused by the combination of linkers and metal centers (in MOFs) or the condensation of building blocks (for COFs). Namely, the separated components of these reticular materials are not able to perform photocatalytic transformations. In other cases, a judicious predesign of photoactive building blocks has been also carried out, consisting on porphyrin [63], thiophene [64], triazine [65], benzoxazole [66], and triphenylamine units [67], among others (Figure 7).

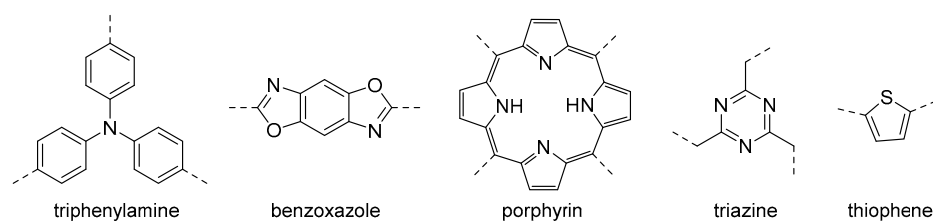


**Figure 7.** Photoactive incorporated linkers in pristine COFs.

## 2.2. Functionalized Materials

The porous structure of reticular materials, in combination with the presence of electron-rich heteroatoms (such as O and N) and long  $\pi$ -conjugated surfaces has allowed the entrapment and functionalization of such organic frameworks with different photocatalysts by means of covalent bonds or supramolecular interactions.

In this sense, for MOFs, the covalent anchorage of different photosensitizers (Vitamin B2 [68], BODIPY [69], Eosin Y [70] or subphthalocyanine [71]) has allowed the obtaining of heterogeneous photocatalysts that generally present higher stability and photocatalytic activity than their homogeneous versions (Figure 8). This enhancement can be due to the immobilization and isolation of photocatalytically active species, hampering unproductive encounters between photoexcited intermediates and, sometimes, leading to a change on the reaction mechanism.



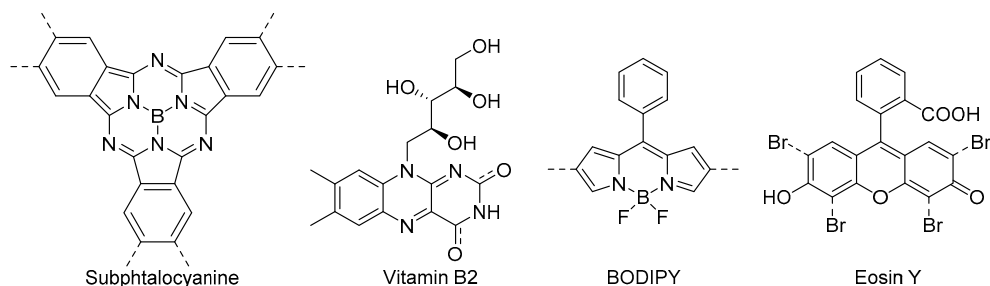
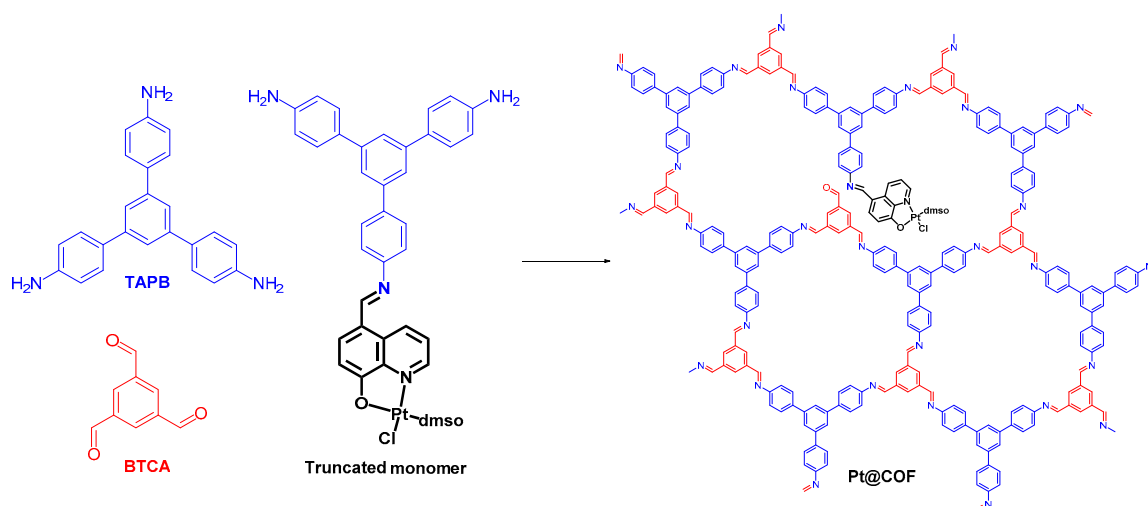


**Figure 8.** Photosensitizers employed in the functionalization of MOFs.

In the case of COFs, this strategy has only been explored in one case by our group, where  $\text{Pt}^{\text{II}}$ -hydroxyquinoline complexes were immobilized and isolated as defects into the porous structure of an imine-based layered COF through monomer truncation strategy (Scheme 2) [72].



**Scheme 2.** Monomer truncation strategy applied in the Pt-functionalization of imine-based COFs.

On another level, the encapsulation of both organic and inorganic homogeneous photocatalysts has also been explored for MOFs, as a result of different supramolecular interactions. For example, taking benefit from the adequate size of the pores and possible  $\pi$ -stacking interactions,  $\text{Ru}^{\text{II}}$  and  $\text{Au}^{\text{III}}$  complexes were occluded into ZIF and MOF structures, by Zhang [34] and Su [73], respectively (Figure 9). In other case, Zhou [42] reported that the cationic  $[\text{Ru}(\text{bpy})_3]^{2+}$  complex was entrapped in the anionic porous structure of PCN-99 MOF through ionic interactions. This sub-strategy has not been evaluated yet in obtaining photocatalytic COFs for organic transformations.

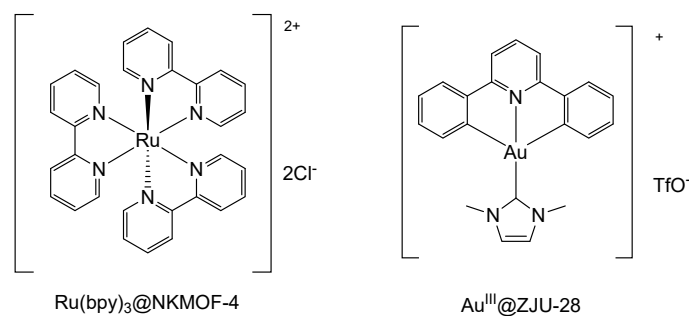


**Figure 9.** Encapsulated photocatalysts in the porous structure of different MOFs.

### 2.3. Hybrid Materials

The integration between reticular organic frameworks and different functional materials can give rise to new opportunities in the synthesis of interesting high-performance composites. These new hybrid materials can combine the abilities and properties of the different components, reaching different reactivity modes and interesting photophysical properties.

In particular, the combination between porous organic frameworks and metal-nanoparticles (NPs) is highly versatile. The variation of the nanoparticle composition, size, shape or environment implies a change on its absorption and emission properties, due to localized surface plasmon resonance (LSPR) phenomena [2]. The deposition of NPs on MOF or COFs surface can improve charge separation, driving electrons from the porous material to the nanoparticles, and increasing the photocatalytic efficiency. The obtaining of this type of hybrid materials can be performed through three different processes: (a) an in situ synthesis, where the material grows in presence of the NP-source; (b) an impregnation methodology, where the bulk material is immersed in a well-dispersed source of NPs; or (c) a controlled-reduction process, where molecular metal precursors are deposited and furtherly reduced to afford the desired NPs hybrid framework (Figure 10).

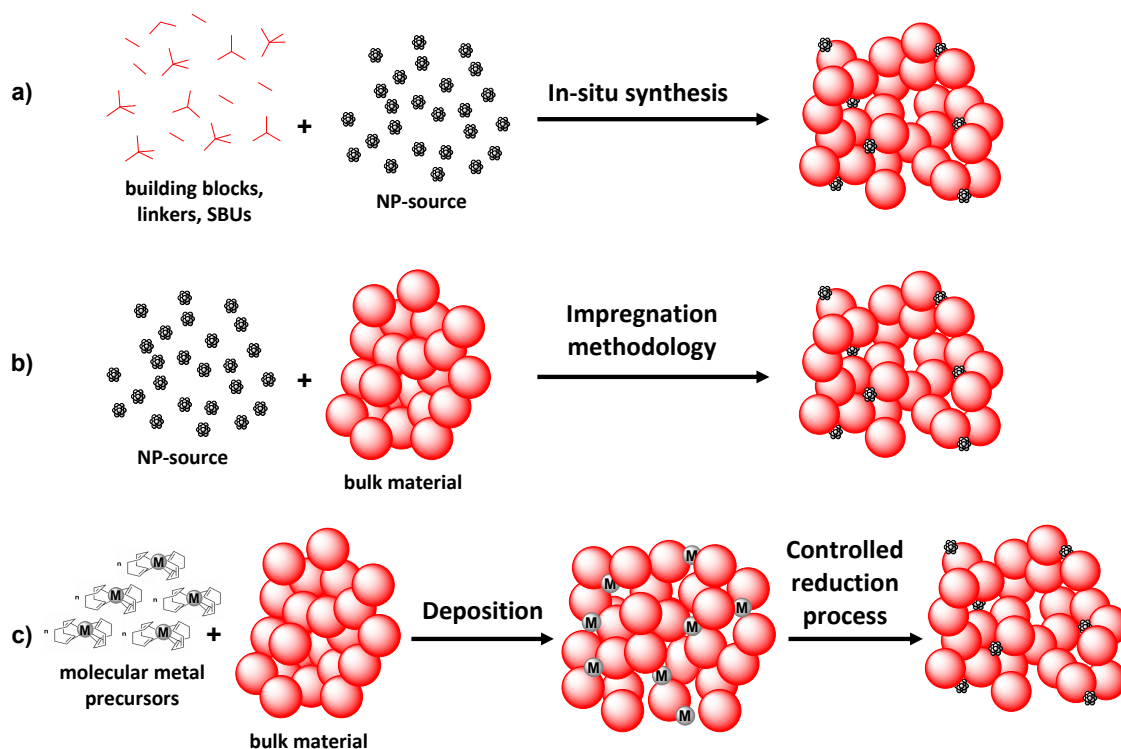


**Figure 10.** Synthetic strategies of hybrid materials with metal NPs: (a) In-situ synthesis. (b) Impregnation methodology. (c) Controlled-reduction process.

On the one hand, in the field of MOFs, different examples of NPs–MOF as photocatalysts for organic transformations can be found, using various metal precursors: Au [74], Ni [75], Pd [76], Pt [77], Pd–Au [78], and Pd–Cu [79]. Most of them are devoted to their use as photocatalysts in the selective oxidation of benzylic alcohol and other oxidation processes (see in more detail below). Apart from MOF–NPs, other hybrid materials have been obtained in this field by using CdS quantum dots [80], bismuth ferrite [81], graphene oxide [82], fullerene C<sub>60</sub> [83], and polyoxometalates [48] as composite partners.

On the other hand, in the field of COFs, only two hybrid materials have been evaluated as photocatalysts for organic transformations: MOF–COF and TiO<sub>2</sub>–COF composites, both reported by Wang’s group [84,85]. In both cases, the strategy consists on using a NH<sub>2</sub>-functionalized material,



in order to facilitate the covalent linkage between the MOF/TiO<sub>2</sub> and the growing imine-based COF. Otherwise, no contributions of NPs–COF composites as photocatalyst for organic transformations have been reported up to now, but other applications, such as hydrogen production, CO<sub>2</sub>-photoreduction or degradation of organic pollutants have been evaluated [9].

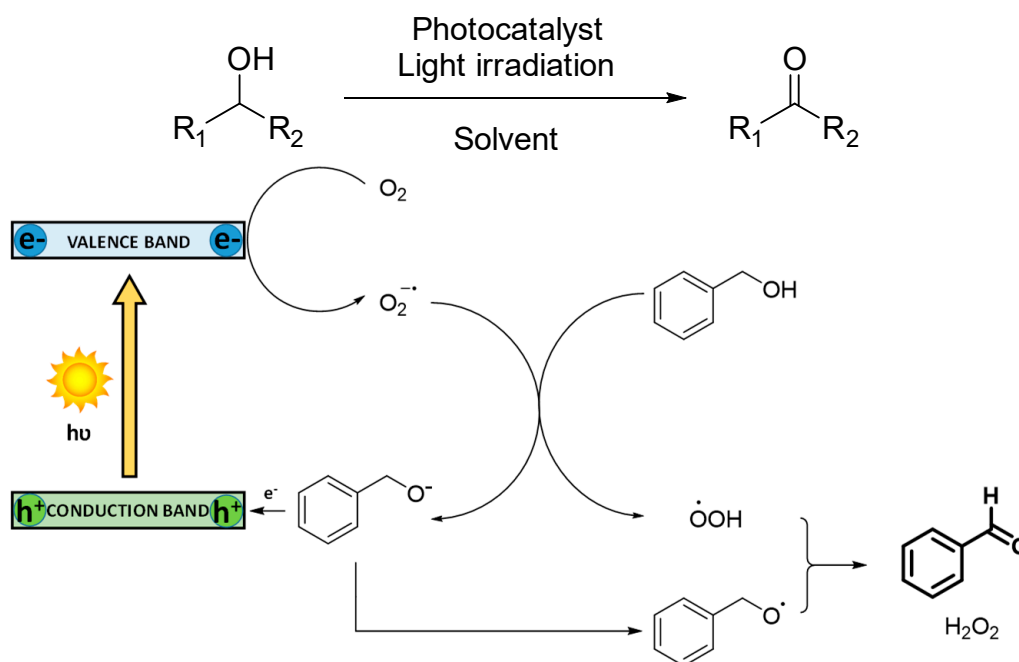
### 3. Organic Reactions

#### 3.1. Oxidation Reactions

Photocatalytic oxidation reactions are chosen for the synthesis of a large number of molecules such as alcohols, epoxides, aldehydes, and ketones. Hazardous oxidizing reagents such as potassium permanganate and dichromate have traditionally been employed in the oxidation of different substrates, producing harmful byproducts. In contrast, aerobic oxidations are presented as an alternative. The development of heterogeneous photocatalytic systems using molecular oxygen as final oxidant leads to greener and more sustainable processes [11]. There are many examples of organic oxidation transformations carried out by MOFs or COFs, as we explain below.

##### 3.1.1. Selective Oxidation of Alcohols

In the selective oxidation of alcohols to aldehydes or ketones, a mechanism based on the generation of superoxide radical anion is commonly reported (Scheme 3). In this case, the photocatalyst absorbs light, and in its excited state, separation of charges is produced, promoting electrons to the conduction band and generating holes in the valence band. These electrons activate O<sub>2</sub> to generate superoxide radical anion (O<sub>2</sub><sup>•−</sup>), which deprotonates benzyl alcohol obtaining hydroperoxide radical species (·OOH). Photogenerated holes are quenched by the benzoxide anion to oxidize it to its radical form, which subsequently reacts with ·OOH, generating benzaldehyde as the final product. H<sub>2</sub>O<sub>2</sub> is also usually produced. Although singlet oxygen is rarely reported, an energy transfer mechanism is observed in some photocatalytic materials, such as Bi-based MOFs. In this case, the presence of Bi suppresses the generation of O<sub>2</sub><sup>•−</sup> and H<sub>2</sub>O<sub>2</sub>, being singlet oxygen the only active oxygen species [55].



**Scheme 3.** Generally accepted mechanism for the oxidation of alcohols. The proposed system consists of benzylic alcohol oxidation which has been the most explored system in the literature.

*Photocatalytic oxidation of alcohols mediated by MOFs* (Table 1): the first example using the design of linkers or SBUs with photoactive fragments was reported in 2011 by Wu [29]. A Sn<sup>IV</sup>-porphyrin-based MOF was capable of oxidizing 1,5-dihydroxynaphthalene to the corresponding quinone with full conversion. In 2012, an outstanding versatile amine-functionalized zirconium MOF, **UiO-66-NH<sub>2</sub>** was used as photocatalyst in various oxidation reactions by Wang and coworkers. Although high catalyst loadings were needed, this report represents the first example where the introduction of amino groups into the constituting linkers of a MOF allowed its use as heterogeneous photocatalyst for several oxidation reactions [86]. This approach was later employed on a series of **UiO-66-NH<sub>2</sub>** derivatives (consisting on mixed-linker zirconium-based MOFs synthesized through a one-pot procedure) which afforded the carbonylic products with moderate conversions [87]. Two years later, the variation of the photocatalytic activity of **MIL-125** as a model platform was studied as a function of the presence of relative amounts of bdc-NH<sub>2</sub> linkers. The oxidation of different alcohols was carried out in order to demonstrate that the maximum photocatalytic activity was achieved with a 50% of bdc-NH<sub>2</sub>, being the amination of all linkers in the MOF not required [88]. In 2019, another three examples employing this strategy were reported. Two bismuth-based MOFs, **Bi-TATB** and **Bi-BTC**, afforded the product in moderate conversions after 5 h [55]. On the other hand, a series of **Ce-UiO-66** MOFs were synthesized with a solvent-free route, achieving the oxidation of alcohols under oxygen flux and near-ultraviolet light irradiation [89]. In addition, a further report demonstrated that was also possible the use of visible-light irradiation in these photocatalytic systems [90].

**Table 1.** Photooxidation reactions of alcohols mediated by MOFs.

Reactants	MOF	Strategy	Light	Power <sup>1</sup> (W)	Reference
Hydroxynaphthalene	Sn <sup>IV</sup> -Porphyrin 3D-MOF(Zn)	Pristine	Xe lamp	350	[29]
Alcohols, olefins, cycloalkanes	UiO-66-NH <sub>2</sub>	Pristine	420–450 nm	300	[86]
Aromatic alcohols	UiO-66-NH <sub>2</sub>	Pristine	Helical bulb	26	[87]
Aromatic alcohols	MIL-125-NH <sub>2</sub>	Pristine	>415 nm	300	[88]
Aromatic alcohols	Bi-TATB, Bi-BTC	Pristine	Xe lamp	300	[55]
Aromatic alcohols	Ce-UiO-66	Pristine	355 nm	-	[89]
Aromatic alcohols	Ce-UiO-66	Pristine	>400 nm	300	[90]
Aromatic alcohols	QUI-MIL-125(Ti)	Functionalization	420–780 nm	-	[91]
Aromatic alcohols	Ru(bpy) <sub>3</sub> @MIL-125-NH <sub>2</sub>	Functionalization	>450 nm	500	[92]
Aromatic alcohols	VB <sub>2</sub> @UiO-66-30	Functionalization	>420 nm	-	[68]
Aromatic alcohols	Au@ZIF-8	Hybrid	>400 nm	-	[74]
Aromatic alcohols	CdS@MIL-100(Fe)-60	Hybrid	>420 nm	500	[80]
Aromatic alcohols	Ni doped NH <sub>2</sub> -MIL-125(Ti)	Hybrid	420–800 nm	300	[75]
Aromatic alcohols	MIL@GO-1%	Hybrid	>420 nm	5	[82]
Aromatic alcohols	0.1%CuO@UiO-66	Hybrid	>400 nm	300	[93]
Aromatic alcohols	BFO/MIL-53(Fe) (BFM-2)	Hybrid	>400 nm	300	[81]

<sup>1</sup> Hyphen indicates that this value is not found in the original report.

Another strategy used to synthesize MOFs capable of oxidizing different type of alcohols consists on the design of functionalization protocols. In 2018, a series of MOFs were structurally altered via post-synthetic modification by the condensation of benzaldehyde molecules with the pending amino groups on **NH<sub>2</sub>-MIL-125(Ti)**. Under visible light irradiation, an enhancement of the photocatalytic activity was achieved by extending the conjugation through this post-synthetic process, carrying out the oxidation of aromatic alcohols with good results [91]. In 2019, the encapsulation of the photoactive [Ru(bpy)<sub>3</sub>]<sup>2+</sup> complex into MIL-125-NH<sub>2</sub> cavities improved its photocatalytic activity in the oxidation of alcohols [92]. Following a different approach, Huang's group carried out the covalent anchorage and isolation of vitamin B<sub>2</sub> into UiO-66. Instead of generating superoxide radical anion via photoredox pathway (as observed for the homogeneous system), **VB<sub>2</sub>@UiO-66** MOF was able

to uniquely give rise to singlet oxygen through an energy transfer process. This effect is due to the immobilization and isolation of  $VB_2$ , hampering triplet-triplet annihilation and increasing the stability of the photocatalyst [68].

Finally, the first reported example of hybrid structures of MOFs capable of performing this oxidation reaction is from 2014. Thus, Duan and coworkers carried out the encapsulation of Au nanoparticles into the porous structure of ZIF-8. The application of epitaxial growth strategy led to single-core shell structures, while the coalescence methodology gave rise to multi-core shell structures (Figure 11). **Au@ZIF-8** composites were employed as heterogeneous photocatalysts for the selective oxidation of a variety of alcohols into the corresponding aldehydes or ketones [74]. One year later, the group of Zhu presented a series of **CdS-MIL-100(Fe)** nanocomposites, formed by the superficial decoration of CdS quantum dots into the corresponding MOFs. The hybrid material presented enhanced photocatalytic activity in comparison with their separated components, because of the increased light absorption efficiency, its superior surface area and the easy charge separation and slow recombination rate. They were capable of oxidizing several alcohols with moderate conversions, reaching up to five consecutive recycling cycles [80]. In 2016, the impregnation of **NH<sub>2</sub>-MIL-125(Ti)** with nickel chloride as a metal source was performed by Zhu [75]. After a reducing treatment with  $NaBH_4$ , Ni nanoparticles were formed. The corresponding **Ni-doped NH<sub>2</sub>-MIL-125(Ti)** was employed as heterogeneous photocatalyst in the selective oxidation of several aromatic alcohols, presenting an enhanced photocatalytic activity as a result of the synergistic effect between Ti–O clusters and Ni–NPs. In 2017, a series of MIL-LIC-1(Eu) graphene oxide composites **MIL@GO** were reported, yielding the final products with good conversions and short reaction times upon visible light irradiation and aqueous media. In this case, according to the authors, the molecular oxygen necessary for the transformation was generated in situ from water [82]. In 2019, the encapsulation and the deposition of copper nanoparticles on a copper-based UiO-66, **Cu/Cu@UiO-66**, was reported. This hybrid material achieved the corresponding oxidized products after 3 h in moderate conversions [93]. Very recently, a very active photocatalytic material has been reported by Yin [81]. The etching and regrowth process on a **3D MIL-53(Fe)**, that generates bismuth ferrite (BFO) nanosheets on its surface, was used as a strategy in order to avoid fast electron–hole recombination.

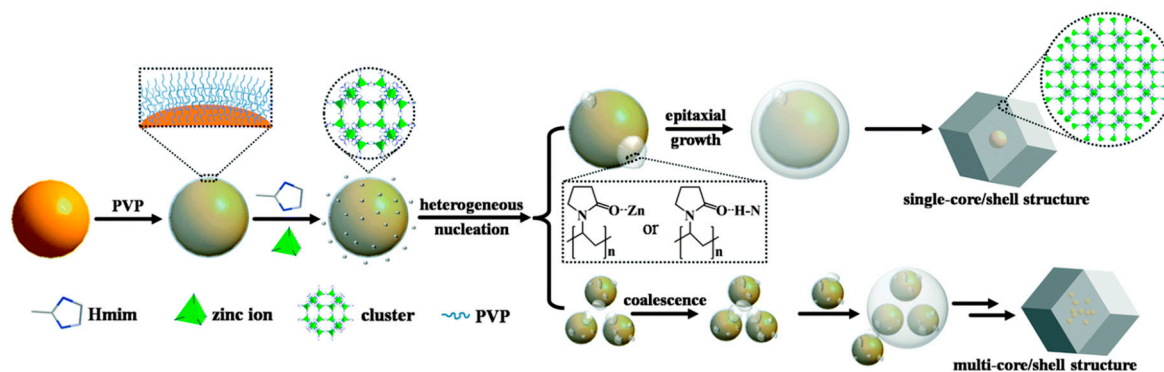


**Figure 11.** Encapsulation of Au-NPs into ZIF-8. Adapted with permission from Reference [74] from The Royal Society of Chemistry.

*Photocatalytic oxidation of alcohols mediated by COFs (Table 2):* The use of COFs as photocatalysts in organic oxidation reactions is still underexplored and most of the works are very recent. The first report is dated to 2017, where an undecorated pristine thiophene-containing CTF (**CTF-Th@SBA-15**) was constructed using mesoporous silica as template. In this work, the performance of this heterogeneous photocatalyst was comparable to the most used non-metal-based catalysts reported up to that date, reaching a similar turnover frequency [64]. The only two examples of hybrid COFs as heterogeneous photocatalysts for synthetic organic transformations using as model reaction the oxidation of alcohols

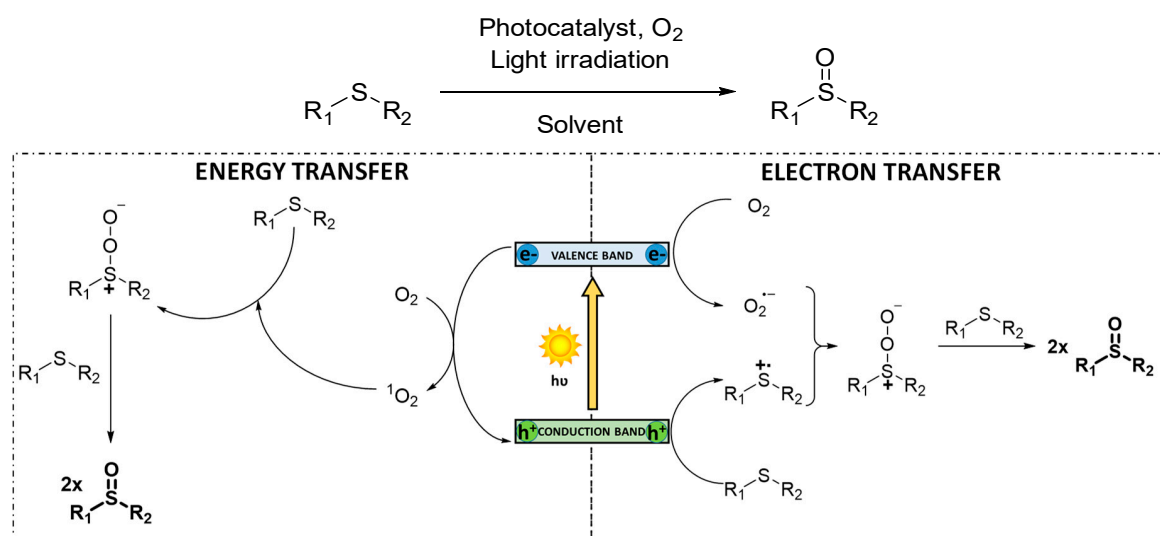
were reported by Wang and coworkers [85]. The first of them was devoted to the coating of TiO<sub>2</sub> nanobelts, with an imine-based COF, obtaining the hybrid material TiO<sub>2</sub>@COF-3. This material presents an enhanced photocatalytic activity due to the improvement on photon absorption related to the possibility of charge transfer from COF to TiO<sub>2</sub>. Such effect makes possible to perform benzylic alcohol oxidation under visible light irradiation. On the other hand, in 2020, a hybrid MOF-COF, NH<sub>2</sub>-MIL-125@TAPB-PDA-3, shown similar photocatalytic properties. In this case, amino groups of the previously synthesized MOF served as linking points to the growth of the imine-based COF [84].

**Table 2.** Photooxidation reactions of alcohols mediated by COFs.

Reactants	COF (Linkage)	Strategy	Light	Power (W)	Reference
Aromatic alcohols	CTF-Th@SBA-15 (triazine-based)	Pristine (photoactive building block)	460 nm	12	[64]
Aromatic alcohols	TiO <sub>2</sub> @COF-3 (imine-based)	Hybrid	420–780 nm	5	[85]
Aromatic alcohols	NH <sub>2</sub> -MIL-125@TAPB-PDA-3 (imine-based)	Hybrid	420–780 nm	5	[84]

### 3.1.2. Selective Sulfoxidation Reactions

Sulfoxides are very interesting compounds since they are prevalent structures in agriculture and pharmaceutical industries [94]. Thus, the selective oxidation of sulfides to sulfoxides is a recurrent model reaction in organic synthesis, since it allows to simply evaluate the photocatalytic activity of the new materials synthesized. Sulfoxidation also allows easy determination of chemoselectivity and to differentiate between the two possible mechanisms involved: an electron transfer or an energy transfer [62] (Scheme 4). On the one hand, in an electron transfer mediated mechanism, charge separation is produced in the photocatalyst under light irradiation. The generated holes oxidize the sulfide to its corresponding cationic radical and the photogenerated electrons reduce O<sub>2</sub> to O<sub>2</sub><sup>•−</sup>. Finally, this active oxygen species reacts with the cationic radical intermediate, generating the persulfoxide species which reacts with a second sulfide to form two molecules of the final sulfoxide. On the other hand, energy transfer process can also take place under visible light irradiation, converting <sup>3</sup>O<sub>2</sub> into <sup>1</sup>O<sub>2</sub> through triplet–triplet annihilation between the triplet excited state of the catalytic fragment and <sup>3</sup>O<sub>2</sub>. Then, singlet oxygen reacts with the organic sulfide generating the same persulfoxide intermediate, which account for the formation of the corresponding sulfoxide product. The occurrence of one or another pathway can be precluded using selective scavengers (e.g., DABCO for singlet oxygen [95], 1,4-dimethoxybenzene for superoxide radical anion [96]). Such mechanistic probes have also been essayed for other oxidation processes. Interestingly, in many cases, there is not an exclusive pathway, and both mechanisms can be simultaneously operative. In some reports, the question of which mechanism produces the sulfoxide product is not addressed.



**Scheme 4.** Mechanism of oxidation of sulfides. At left, energy transfer mechanism, where singlet oxygen is the reactive oxygen species. At right, electron transfer mechanism, where superoxide radical anion is the reactive oxygen species.

*Photocatalytic selective oxidation of sulfides mediated by MOFs* (Table 3): Focusing on the field of MOFs, there are some examples in which the design of linkers or SBUs with photoactive fragments is the chosen strategy. In 2011, the versatile Sn<sup>IV</sup>-porphyrin-based MOF previously presented in the alcohol oxidation part was also able to oxidize sulfides to sulfoxides with good results. In addition, the process became more selective by the immobilization of porphyrinic fragment (that acts as photosensitizer) into the porous framework, without overoxidation into sulfone product. In contrast, sulfone is found when the analogous molecular porphyrin was employed [29]. In the same year, Lin and coworkers reached the obtaining of bimetalated MOFs, by doping of UiO-67 with Ir, Re and Ru centers through the combination of both pre-synthesized metal-coordinated and naked linkers with Zr nodes. These doped MOFs were used as photocatalyst in the selective photosulfoxidation reaction, among other model test reactions, proposing an energy transfer mechanism [59]. Three years later, an anionic indium porphyrin framework, UNLPP-10, was capable of selectively oxidizing sulfides under low power visible light irradiation [31]. In 2019, three bimetallic Ir<sup>III</sup>-Zr<sup>IV</sup> MOFs were synthesized (**Zr<sub>6</sub>-Irbpy**, **Zr<sub>6</sub>-IrbpyOMe**, and **Zr<sub>6</sub>-Irphen**) by the combination of predesigned Ir-phenylpyridine complexes as ancillary linkers and Zr as metal nodes. Their extreme stability allowed the use of water as solvent in the sulfoxidation tests, observing a photoredox pathway as the preferred reaction mechanism. In addition, the **Zr<sub>6</sub>-Irphen** catalyst was recycled up to 10 times without losing its effectivity, neither its structural integrity (Figure 12). [35]. The same exclusive photoredox activity was observed for an anthracene-based MOF, NNU-45, that was lately reported [36].

**Table 3.** Photosulfoxidation reactions mediated by MOFs.

Reactants	MOF	Strategy	Light	Power (W)	Reference
Sulfides	Sn <sup>IV</sup> -Porphyrin 3D-MOF(Zn)	Pristine	Xe lamp	350	[29]
Sulfides	UNLPP-10	Pristine	465 nm	0.135	[31]
Sulfides	Zr <sub>6</sub> -Irphen	Pristine	Blue	100	[35]
Sulfides	NNU-45	Pristine	>420 nm	300	[36]
Sulfides	3%-C <sub>60</sub> @PCN-222	Hybrid	>400 nm	50	[83]



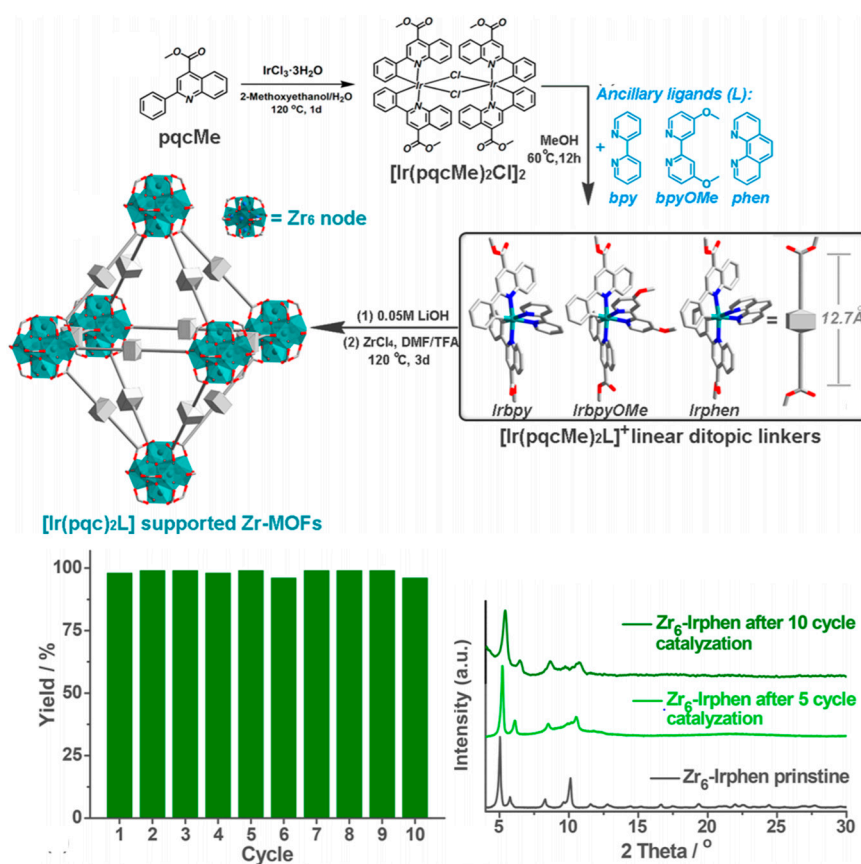


**Figure 12.** Structural design and photocatalytic application of Zr–Ir–MOFs into sulfoxidation processes. Adapted with permission from Reference [35], Copyright (2019) American Chemical Society.

The last example consists on a hybrid MOF obtained by the integration of guest  $C_{60}$  molecules and a porous porphyrin-based MOF,  $C_{60}@PCN-222$ , which selectively achieved sulfoxides [83]. This composite takes advantage of the special properties of fullerene  $C_{60}$ , due to the fact of its highly delocalized conjugated structure that accounts for the generation of reactive oxygen species. In particular, the high electron affinity of  $C_{60}$  is a key factor to enhance photoinduced charge separation with slow recombination. Thus, the combination of fullerenes with semiconductor MOFs resulted in an increased photocatalytic activity.

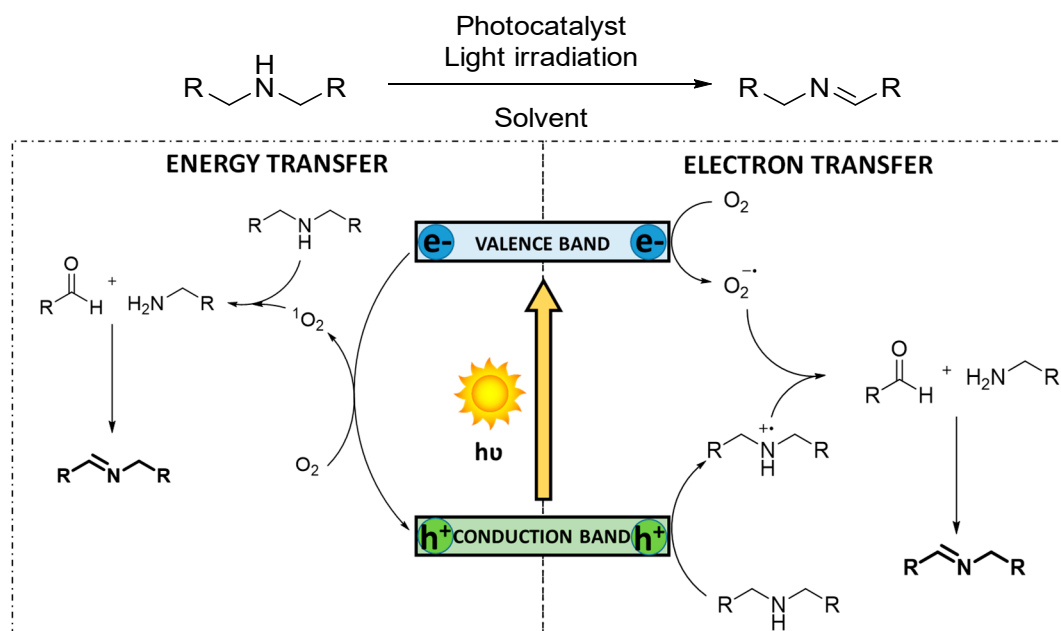
*Photocatalytic selective oxidation of sulfides mediated by COFs* (Table 4): Our research group published in 2019 three different undecorated imine-based pristine materials: a layered-COF, a spherical-COF, and a 3D-COF that demonstrated photocatalytic activity in oxidation reactions. In particular, the oxidation of sulfides to sulfoxides efficiently proceeded using an ecofriendly mixture of solvents (ethanol and water) [62]. Remarkably, despite the use of water as a solvent, imine-based COFs were stable enough to perform several consecutive catalytic runs without losing activity. In the same year, two  $N,N'$ -bicarbazole-based CTFs, **BC-CTF** and **Ph-BC-CTF**, carried out the same oxidation reactions [97]. Very recently, a 2D and a 3D Pd-containing porphyrinic COFs, **2D-PdPor-COF** and **3D-PdPor-COF**, were capable of oxidizing the sulfides in very short reaction times (25 min), using low power visible light irradiation [98]. Also, a nanostructured COF, **h-LZU1**, which was obtained by using nanocrystals of ZIF-8 as template to yield capsule structures was obtained. This material was reported as photocatalytically active towards sulfoxidation under high power light UV-Visible irradiation with low recyclability and not complete selectivity [99]. Finally, our group reported the covalent in situ anchorage of photoactive  $Pt^{II}$ -hydroxyquinoline complexes as defects into imine-based COFs, presenting TON up to 8000 and good stability and recyclability in comparison with molecular complex and pristine material [72].

**Table 4.** Photosulfoxidation reactions mediated by COFs.

Reactants	COF (Linkage)	Strategy	Light	Power (W)	Reference
Sulfides	Laminal COF (imine-based)	Pristine (undecorated)	450 nm	15	[62]
Sulfides	BC-CTF (triazine-based)	Pristine (photoactive building block)	>400 nm	300	[97]
Sulfides	2D or 3D-PdPor-COF (imine-based)	Pristine (photoactive building block)	Blue	3	[98]
Sulfides	h-LZU1 (imine-based)	Pristine (undecorated)	>380 nm	300	[99]
Sulfides	Pt@COF	Functionalization	450 nm	15	[72]

### 3.1.3. Photocatalytic Dehydrogenation of Secondary Amines

The selective oxidative dehydrogenation of secondary amines to imines is feasible, due to the stability of the products and the impossibility of the substrates to generate nitriles. However, the substrate conversion is influenced by the steric hindrance around the N–H bond. In addition, the chemoselectivity for the oxidation of asymmetric dibenzylamines is often hampered because two different  $\alpha$ -CH bonds can lead to distinct products. Therefore, examples of oxidation of symmetric dibenzylamines are common, while the selective oxidation of asymmetric dibenzylamines still remains challenging. The mechanism of the reaction has been reported for both reactive oxygen species,  $O_2^{\cdot -}$  and  $^1O_2$  [46,73] (Scheme 5). In the first case, superoxide radical anion is concomitantly formed to the amine radical cation species. Such activated intermediates furtherly react triggering heterolytic cleavage, generating a mixture of benzaldehyde and benzylamine, which ultimately condensate to the corresponding imine. For the energy transfer mechanism, the singlet oxygen species directly reacts with the amine, provoking the subsequent heterolytic cleavage.

**Scheme 5.** Photocatalytic oxidation reaction of secondary amines to imines.

*Photocatalytic oxidation of amines into imines mediated by MOFs* (Table 5): A pristine zinc-based MOF containing anthracene linkers as photosensitizers was reported in 2019, carrying out the photooxidation of secondary amines to the corresponding imines in short reaction times and great yields [46]. A different strategy, which is related to the encapsulation of photoactive Au complexes into the porous structure of two MOFs, was achieved by Su and collaborators. The isolation and immobilization of emissive Au



complexes into  $\text{Au}^{\text{III}}@ \text{MOF1}$  and  $\text{Au}^{\text{III}}@ \text{ZJU-28}$  resulted on the improvement of emission intensity, quantum yield, life-time of the excited state, and selective photocatalytic activity with respect to the complex in solution [73].

**Table 5.** Photooxidation reactions of secondary amines mediated by MOFs.

Reactants	MOF	Strategy	Light	Power (W)	Reference
Secondary amines	Anthracene 3D-MOF(Zn)	Pristine	>420 nm	300	[46]
Secondary amines	$\text{Au}^{\text{III}}@ \text{ZJU-28}$	Functionalization	>300 nm	300	[73]

*Photocatalytic oxidation of amines into imines mediated by COFs* (Table 6): A very stable 2D porphyrin-containing COF, **Por-sp<sup>2</sup>c-COF**, was synthesized by Wang and collaborators [63] through the Knoevenagel condensation, giving rise to a cyanovinylene-based COF. This material was firstly used to generate the imine products in only 30 min under low power visible light irradiation. In 2020, they also reported that the same **Por-sp<sup>2</sup>c-COF** was also capable of oxidizing secondary amines in combination with TEMPO as co-catalyst in 18 min using low-power red light source through a two-photon absorption mechanism [28].

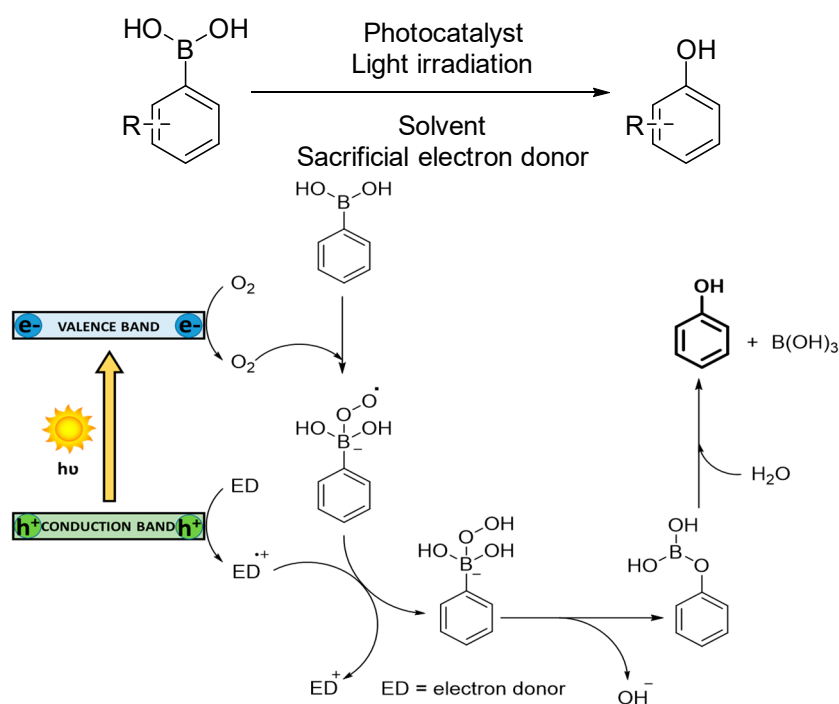
**Table 6.** Photooxidation reactions of secondary amines mediated by COFs.

Reactants	COF (Linkage)	Strategy	Light	Power (W)	Reference
Secondary amines	Por-sp <sup>2</sup> c-COF (cyanovinylene-based)	Pristine (photoactive building block)	White LED	3	[63]
Secondary amines	Por-sp <sup>2</sup> c-COF (cyanovinylene-based)	Pristine (photoactive building block)	623 nm	3	[28]

#### 3.1.4. Oxidation of Arylboronic Acids

The oxidation of arylboronic acids to phenols is known to proceed exclusively via superoxide radical anion [100]. Charge separation occurs in the photocatalyst under light irradiation, generating holes that oxidize a tertiary amine as sacrificial electron donor to its corresponding cationic radical and the photogenerated electrons reduce  $\text{O}_2$  to  $\text{O}_2^-$ . The transient reactive oxygen species directly reacts with arylboronic acid, forming an anionic radical intermediate. This radical species abstracts one hydrogen atom from the cationic oxidized amine. Finally, an irreversible rearrangement ion migration ( $\text{OH}^-$ ) is subsequently followed by a hydrolysis affording the final phenol (see Scheme 6).

*Photocatalytic oxidation of arylboronic acids mediated by MOFs* (Table 7): In 2015, two research groups, Matsuoka and Zhang, reported two different porphyrin-containing MOFs able to oxidize arylboronic acids to phenols. **Zr-MOF-TCPP** (also known as **MOF-525**) achieved the final phenol product under green LEDs irradiation using triethylamine as sacrificial electron donor [101]. In the other case, a family of UNLPF-MOFs were synthesized by varying the amount and the nature of the coordinated metal ( $\text{Sn}^{\text{II}}$ ,  $\text{Sn}^{\text{IV}}$  or  $\text{In}^{\text{III}}$ ). The photophysical properties of the materials synthesized were evaluated, and further translated into their application as photocatalyst in different organic transformations. As a result of this analysis, it was found that **UNLPF-12** (which contains  $\text{Sn}^{\text{IV}}$  coordinated to the porphyrin and  $\text{In}^{\text{III}}$  as metal node) was the optimal photocatalyst for the oxidative hydroxylation of different substituted arylboronic acids [32].



**Scheme 6.** Mechanism of the photooxidation of arylboronic acids.

**Table 7.** Photooxidation reactions of arylboronic acids mediated by MOFs.

Reactants	MOF	Strategy	Light	Power (W) <sup>1</sup>	Reference
Arylboronic acids	(MOF-525)	Pristine	523 nm LEDs	-	[101]
Arylboronic acids	UNLPPF-12	Pristine	CFL	14	[32]
Arylboronic acids	UiO-67-[Ru(bpy) <sub>3</sub> ] <sub>0.1</sub>	Functionalization	365 nm	-	[102]
Arylboronic acids	Ru(bpy) <sub>3</sub> @PCN-99	Functionalization	Fluorescence lamp	36	[42]

<sup>1</sup> Hyphen indicates is value was not found in the original report.

Functionalization processes related to the different incorporation of [Ru(bpy)<sub>3</sub>]<sup>2+</sup> complexes are also described in this reaction. In 2015, Cohen reported a UiO-67-based MOF with coordinated Ru centers (**UiO-67-Ru(bpy)<sub>3</sub>**). This material was capable of oxidizing arylboronic acids under near-UV and visible light irradiation with DIPEA as sacrificial electron donor [102]. In this case, the complex is covalently bonded to the material, since the linker contain bipyridine ligands. One year later, a different strategy was applied by Zhou [42], consisting on the occlusion of molecular [Ru(bpy)<sub>3</sub>]<sup>2+</sup> that established coulombic interactions with the anionic indium-based MOF, **PCN-99**. This functionalized framework was able to catalyze the oxidation of arylboronic acids, using also diisopropylethylamine (DIPEA) as sacrificial electron donor.

*Photocatalytic oxidation of arylboronic acids mediated by COFs* (Table 8): in 2018, three new benzoxazole-linked COFs, (**LZU-190** to **192**), were obtained by Wang and coworkers [66] through cascade-type reactions (see Figure 13). The initially imine-based formed COF evolved to the corresponding benzoxazole linkage thanks to the hydroxyl groups present in the amine-containing building block, conferring an outstanding stability to the material. This stability was confirmed by running until 20 photocatalytic cycles in the oxidation of phenylboronic acids to phenols with full conversion in each cycle. A different approach was employed in 2019, where an imine-linked COF was obtained through the self-condensation of a tetratopic building block, which contains both

aldehydes and amino groups into its structure. The **BBO-COF** achieved the corresponding phenolic product with quite long reaction times [97]. Finally, three imine-based undecorated COFs with different architectures and morphologies carried out the oxidation of phenylboronic acid to phenol using a household white bulb as irradiating system with moderate yields, confirming the photoredox activity of these materials [62].

**Table 8.** Photooxidation reactions of arylboronic acids mediated by COFs.

Reactants	COF (Linkage)	Strategy	Light	Power (W) <sup>1</sup>	Reference
Arylboronic acids	LZU-190 (benzoxazole-based)	Pristine (photoactive linkage)	White LED	20	[66]
Arylboronic acids	BBO-COF (imine-based)	Pristine (photoactive building block)	White	18	[97]
Arylboronic acids	Imine-based COFs	Pristine (undecorated)	White	-	[62]

<sup>1</sup> Hyphen indicates that this value was not found in the original report.

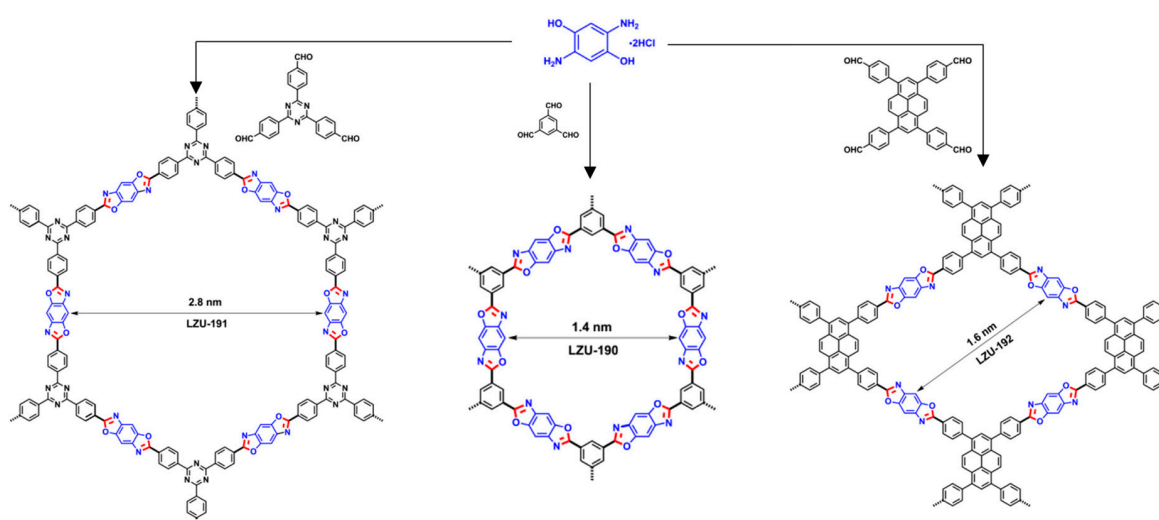


**Figure 13.** Design of benzoxazole-linked COFs. Adapted with permission from Reference [66], Copyright (2019) American Chemical Society.

*Other photocatalytic oxidation reactions mediated by MOFs (Table 9):* In addition, there are some examples of oxidation reactions that have only been carried out using MOFs, remaining unexplored in the field of COFs. The first example dates from 2012, where large catalytic loadings of **UiO-66-NH<sub>2</sub>** were employed to achieve the oxidation of cyclohexane to cyclohexanone and epoxidation of cyclooctene and styrene derivatives. They described the mechanism of these transformations as an electron transfer process through the oxidation of the hydrocarbon concomitantly with superoxide radical anion formation. Such mixture of transient species eventually evolved to the corresponding products [86].

**Table 9.** Various photooxidation reactions mediated by MOFs.

Reactants	MOF	Strategy	Light	Power (W) <sup>1</sup>	Reference
Alcohols, olefins, cycloalkanes	UiO-66-NH <sub>2</sub>	Pristine	420–450 nm	300	[86]
Benzene	MIL-100(Fe)	Pristine	420–800 nm	300	[54]
Benzyl halides	Ru(bpy) <sub>3</sub> @NKMOF-4	Functionalization	White	-	[34]
N-alkylquinolinium salts	Pt <sub>0.9</sub> @PCN-221	Hybrid	425 nm	-	[77]

<sup>1</sup> Hyphen indicates that this value is not found in the original report.

In 2015, two pristine Fe-based MOFs, **MIL-100(Fe)** and **MIL-68(Fe)**, were capable of oxidizing benzene to phenol using a mixture of acetonitrile and water as solvent and H<sub>2</sub>O<sub>2</sub> as reagent [54]. These MOFs produce the homolytic cleavage of hydrogen peroxide to generate active hydroxyl radicals ( $\cdot\text{OH}$ ) and the oxidation of Fe<sup>II</sup> centers, forming Fe<sup>III</sup>-OH species via photo-Fenton-like reaction. The hydroxyl radical attacks the benzene ring to form the hydroxycyclohexadienyl radical, that finally evolves to the phenol product through a hydrogen atom abstraction. This process also leads to the reduction of Fe<sup>III</sup>-OH into Fe<sup>II</sup> and the release of a water molecule, regenerating the original catalytic species (see Figure 14).

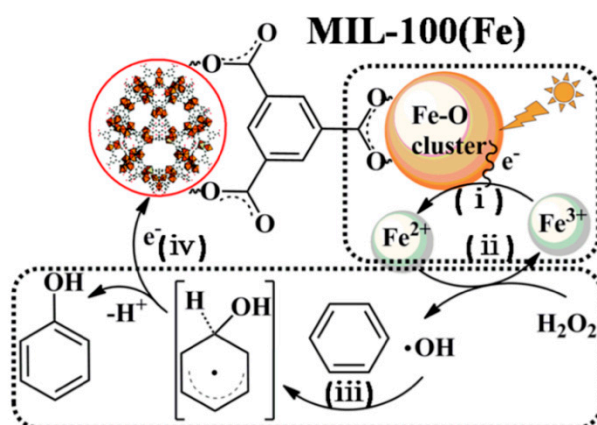
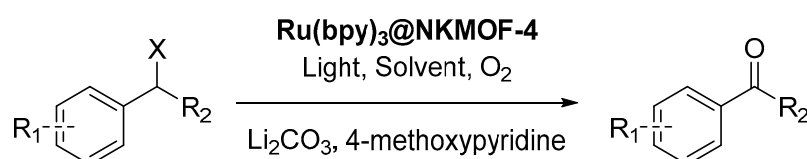


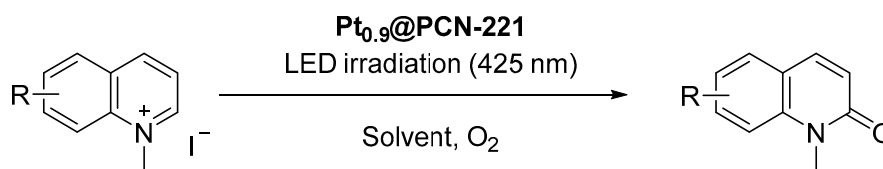
**Figure 14.** Photo-Fenton type mechanism for the hydroxylation of benzene catalyzed by MIL-100(Fe). Adapted with permission from Reference [54], Copyright (2015) American Chemical Society.

In 2019, the encapsulation of [Ru(bpy)<sub>3</sub>]<sup>2+</sup> into the porous structure of a ZIF was performed by Zhang [34]. It was achieved by the *in-situ* construction of the framework in presence of the mentioned complex, allowing the isolation of **Ru(bpy)<sub>3</sub>@NKMOF-4**. The photocatalytic activity of this functionalized material was evaluated using the oxidation of benzyl halides to the corresponding acetophenones as a model reaction (Scheme 7). As co-catalyst, 4-methoxypyridine was used, and Li<sub>2</sub>CO<sub>3</sub> was added as a base under white light irradiation, resulting in the full conversion of various benzyl halides. They proposed a complex mechanistic landscape, in which the superoxide radical anion is involved, and the 4-methoxypyridine acts as electron transfer mediator.



**Scheme 7.** Photooxidation of benzyl halides mediated by Ru(bpy)<sub>3</sub>@NKMOF-4.

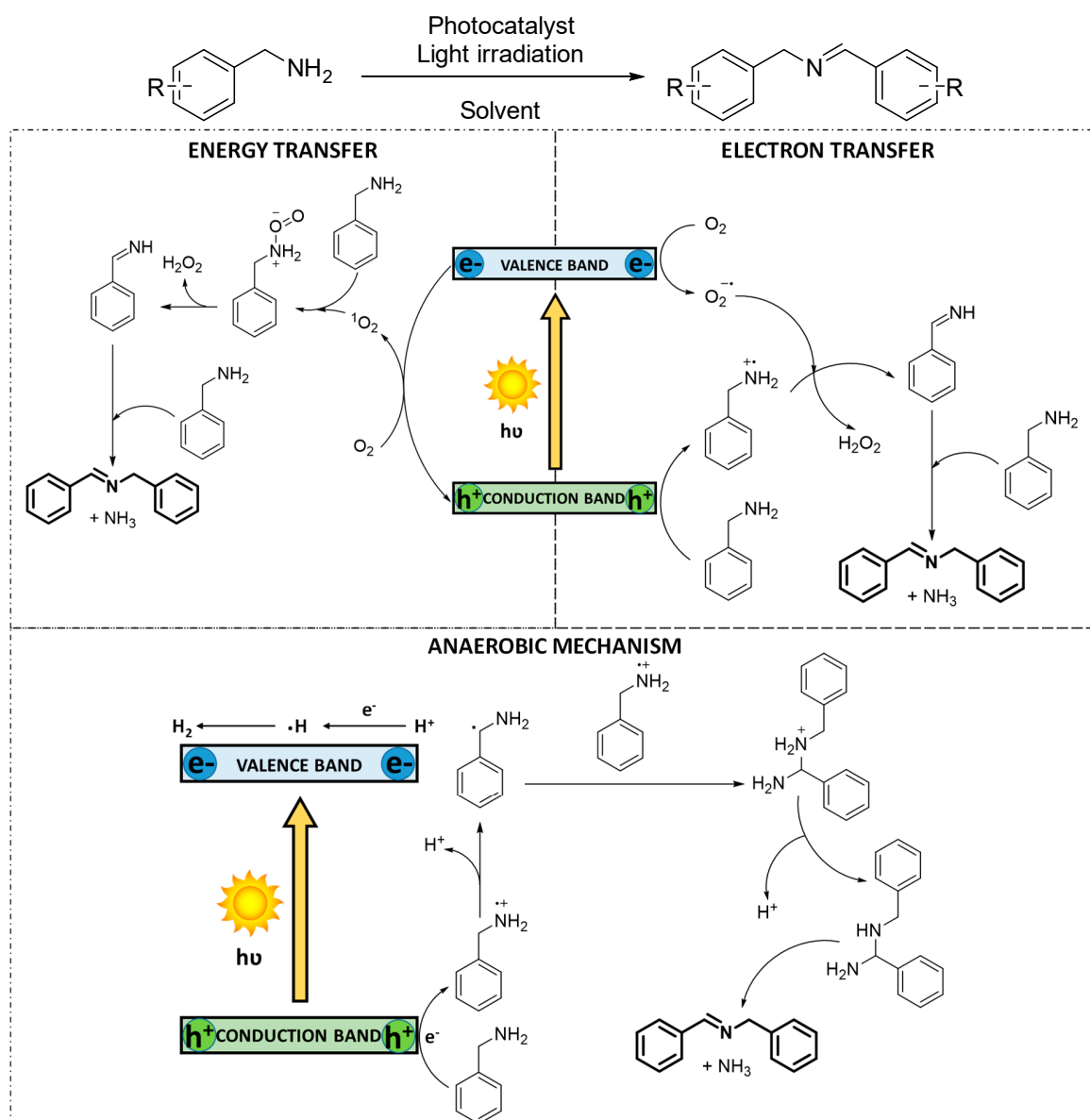
Very recently, the generation of Pt nanoclusters supported on the surface of PCN-221 through photoreduction was achieved. This hybrid material was employed as photocatalyst for the oxidation of different *N*-alkyl(iso)quinolinium halides into the corresponding *N*-alkyl(iso)quinolones via singlet oxygen generation (Scheme 8) [77].



**Scheme 8.** Photooxidation of *N*-alkyl(iso)quinolinium halides by  $\text{Pt}_{0.9}\text{@PCN-221}$ .

### 3.2. Oxidative Coupling

Oxidative couplings are classically catalyzed by a transition metal complex, like in typical cross-coupling reactions, although the mechanism changes because the oxidation process requires an oxidant to keep the entire process electroneutral [103]. In this sense, photocatalytic oxidative coupling reactions emerge as an alternative to make more sustainable processes than classical cross-coupling reactions. The two nucleophilic centers are often bound to hydrogen atoms, which makes possible hydrogen atom abstraction/transfer processes that are crucial in the general mechanism. The oxidative process transforms one of the nucleophiles into an electrophile, enabling the coupling between two molecules that were initially both of nucleophilic nature. The most common oxidant is  $\text{O}_2$  and the energy source consists on visible light in many cases, which fulfills the requirements of green chemistry. In particular, the selective oxidative coupling of amines to imine derivatives as important building blocks for the synthesis of fine chemicals and pharmaceuticals is highly desired. Photoinduced aerobic oxidation is the most sustainable and effective alternative under moderate conditions, avoiding high temperatures ( $\sim 373$  K) and high oxygen pressures ( $\sim 5$  atm) [104]. In almost all the reported works using reticular materials as photocatalysts, the reaction mechanism runs via electron transfer. However, there are a few published examples that proceed via energy transfer [33]. The electron transfer mechanism (Scheme 9, right) is initially triggered by the electrons promoted to the valence band of the photocatalyst, that are transferred to  $\text{O}_2$ , generating superoxide radical anion ( $\text{O}_2^{\cdot -}$ ). Such process involves the generation of electron holes, that trigger the formation of the amine radical cation (regenerating the original form of the catalyst). Further evolution of this reactive species consists on a hydrogen atom abstraction from the amine radical cation, generating the iminium cation and  $\text{HO}_2^-$  species. Subsequent proton transfer accounts for the formation of imine intermediate and hydrogen peroxide byproduct. Such imine species furtherly condensates with the excess of amine present in the reaction medium, generating the final coupling product via an aminal intermediate and ammonia as byproduct. In an energy transfer mechanism (Scheme 9, left), the excited state of the photocatalyst can generate  $^1\text{O}_2$  via triplet–triplet annihilation with  $^3\text{O}_2$ . Singlet oxygen is the activated oxygen form causing the formation of imine intermediate and hydrogen peroxide. Overall, the observed byproducts are the same, regardless of the mechanism. Some research has even reached the anaerobic version (Scheme 9, bottom), where protons act as oxidants, generating hydrogen as byproduct [105]. As a result of this electron transfer, electron holes are generated, which also trigger the formation of the amine radical cation transient species. Two molecules of such cationic intermediate can condensate into an aminal species through a double deprotonation process which furtherly evolve to the final product and ammonia.



**Scheme 9.** Possible mechanisms for the oxidative coupling of primary amines.

*Oxidative coupling reactions mediated by MOFs* (Table 10): the most recurrent strategy consists in the design of linkers with photoactive fragments such as anthracene or porphyrin. In 2011, as previously presented in the sulfoxidation section, the doping of UiO-67-like MOFs was performed by Lin and coworkers, allowing the obtaining of bimetalated materials, which were used as photocatalyst in the oxidative coupling of primary benzylamines, among other oxidative transformations [59]. In 2015, a family of different metallated porphyrinic MOFs (see section about oxidation of arylboronic acids for further details) was described. In this case, UNLPF-12 provides a highly oxidative photoexcited state that efficiently performed the oxidative coupling of benzylamines [32]. In 2018, another porphyrinic MOF with Zr-oxo clusters (PCN-222) was reported, presenting comparable photocatalytic activity to the previous published works [104]. Later, two MOFs containing anthracene units as photosensitizers were obtained by Xing's group [36,46], and their photocatalytic activity was evaluated using the oxidative coupling of amines as a model reaction. In the first case, a 3D indium-based MOF (NNU-45) was employed [36], while in the other case, a zinc-based MOF was the chosen one [46]. In the same year, Duan and coworkers [33] obtained a family of Zn-based MOFs that contains different ratios of pyridine and methylpyridinium linkers, ZJU-56, capable of achieving C–N and C–C oxidative coupling reactions



through two-photon absorption processes (see in CDC section). Otherwise, a ligand functionalization protocol of UiO-66 allowed the obtaining of different UiO-66-NH<sub>2</sub> MOFs, that enabled the isolation of the corresponding imine products under both aerobic and anaerobic conditions. [105]. There are also two recent examples of hybrid structures of MOFs capable of performing this organic transformation. In 2019, a MOF decorated with CdS quantum dots was reported (CdS@MIL-101). They obtained imine products from the oxidative coupling of primary amines. In addition, the same product was also obtained by the reaction of phenols with anilines, generating water instead of ammonia as byproduct [106]. Finally, very recently, a hybrid material with an optimal Pd nanocrystals loading, Pd/MIL-125-NH<sub>2</sub>, improved the benzylamine conversion rate of pristine MIL-125-NH<sub>2</sub> [76].

**Table 10.** Photooxidative couplings of primary amines mediated by MOFs.

Reactants	MOF	Strategy	Light	Power (W) <sup>1</sup>	Reference
Aromatic amines	UiO-67-doped (MOF-6)	Pristine	>300 nm	300	[59]
Aromatic amines	UNLPPF-12	Pristine	CFL	14	[32]
Aromatic amines	PCN-222	Pristine	>420 nm	-	[104]
Aromatic amines	NNU-45	Pristine	>420 nm	300	[36]
Aromatic amines	Anthracene 3D-MOF(Zn)	Pristine	>420 nm	300	[46]
Aromatic amines	ZJU-56-0.2	Pristine	660 nm	-	[33]
Aromatic amines	UiO-66-NH <sub>2</sub>	Pristine	Xe lamp	-	[105]
Aromatic amines, phenols and anilines	CdS(2 wt%)/MIL-101	Hybrid	>420 nm	300	[106]
Aromatic amines	Pd <sub>1.0</sub> /MIL-125-NH <sub>2</sub>	Hybrid	360–780 nm	300	[76]

<sup>1</sup> Hyphen indicates that this value was not found in the original report.

*Oxidative coupling reactions mediated by COFs* (Table 11): only two very recent examples have been reported, related to the incorporation of photoactive building blocks into the COF structure in order to be used in this transformation. In the first case, a porphyrin-containing COF (**Por-sp<sup>2</sup>c-COF**) was obtained through the Knoevenagel condensation. It was employed as photocatalyst in combination with TEMPO as co-catalyst and oxygen as the terminal oxidant species, generating the coupling product in less than 30 min and using low power red light source [28]. On the other hand, a hydrazone-based COF (**TFPT-BMTH**) was reported for the oxidative coupling of benzylamine using water as solvent. It is an environmentally friendly process that has shown good recyclability of the catalyst to synthesize imines in good conversions after 24 h of irradiation [65]. It should be noticed that, for this reaction, the use of more stable materials is needed, especially in the field of COFs, since amines are employed as reagents. Apart from their basicity, they are well-known because of their nucleophilicity, which can lead to the destruction of the structural integrity of the material [107]. Thus, leaching and recyclability tests should be mandatory in this type of transformations, in order to ensure and reaffirm the heterogeneity of the catalyst and its stability.

**Table 11.** Photooxidative couplings of primary amines mediated by COFs.

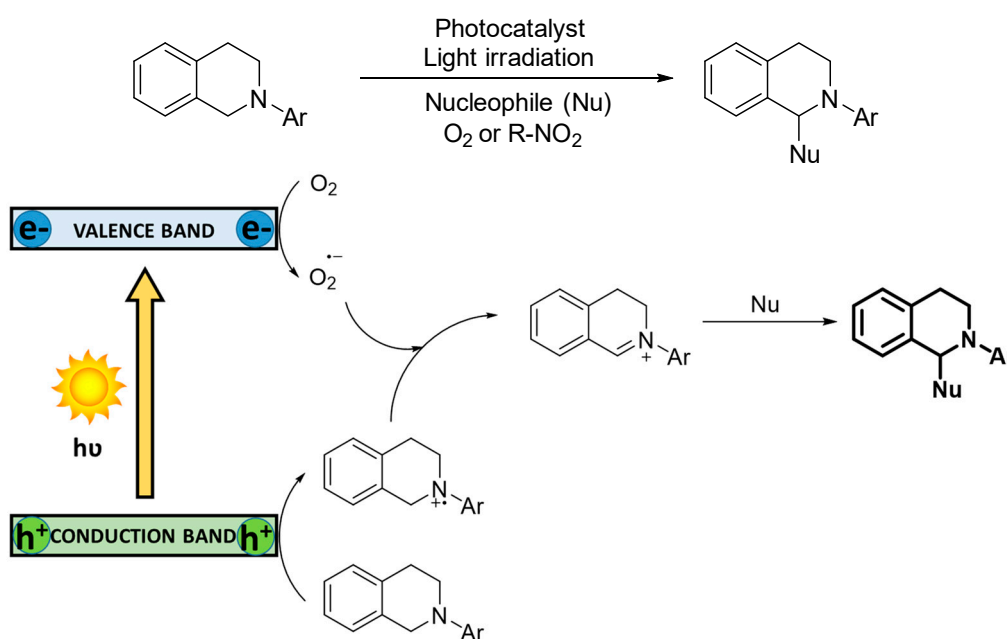
Reactants	COF (Linkage)	Strategy	Light	Power (W)	Reference
Aromatic amines	Por-sp <sup>2</sup> c-COF (cyanovinylene-based)	Pristine (photoactive building block)	623 nm LEDs	3	[28]
Aromatic amines	TFPT-BMTH (hydrazone-based)	Pristine (photoactive building block)	454 nm LEDs	30	[65]

### 3.3. Cross-Dehydrogenative Coupling

An important method to generate new C–C or C–Heteroatom bonds under mild conditions consists on the C–H bond cross-dehydrogenative coupling (CDC). Between all the possible CDC reactions, the functionalization of *N*-aryltetrahydroisoquinolines (THIQs) and other tertiary amines



with different nucleophiles represents one of the most employed photocatalytic tests in order to evaluate the photoredox activity of a high variety of catalytic systems [108]. As coupling partners, a large variety of nucleophiles has been employed, such as malonates, nitriles, phosphites, and nitro-derivatives. The mechanism of this type of transformations has been widely studied [108]. In the case that the reaction proceeds under oxygen atmosphere, the oxygen will act as the terminal oxidant (Scheme 10). In general, the photoexcited catalytic material triggers the reduction of oxygen to superoxide radical anion species, generating the corresponding electron holes which are responsible of oxidation of THIQ into the amine radical cation. This superoxide radical anion can react with the previously generated amine radical cation in order to generate an iminium ion, which is highly electrophilic and reacts with a variety of nucleophiles. In some of the cases, the reaction proceeds in the absence of oxygen, but a super-stoichiometric amount of nitro-derivative as the terminal oxidant (which is also the nucleophile) is needed.



**Scheme 10.** Generally accepted mechanism for cross-dehydrogenative coupling (CDC) reaction.

*Cross-dehydrogenative coupling reactions mediated by MOFs* (Table 12): In the field of MOFs, there are various examples where this reaction has been employed in order to evaluate the photocatalytic activity of this type of materials. The preferred strategy consists on the design of photoactive linkers. For example, in 2011, Lin and coworkers [59] carried out the partial functionalization of **UiO-67** constituted by dicarboxylic matching linkers containing Ir-phenylpyridine and Ru-bipyridine moieties. The **UiO-67-doped** presented high activity towards azaHenry reaction between *N*-aryl-THIQs and nitromethane as solvent. The different **UiO-67-doped** MOFs were also successfully employed as photocatalysts for CO<sub>2</sub>-photoreduction, and several oxidation reactions. Later, in 2015, Zhang et al. [32] reported the synthesis and photocatalytic applications of different UNLPF MOFs. In particular, **UNLPF-12**, which contains Sn<sup>IV</sup>-porphyrin as linker, was able to catalyze CDC between different *N*-aryl-THIQs and acetone as nucleophile. In 2016, Wang and collaborators reported the synthesis of **UiO-68-mtpdc/etpdc**, a MOF that contains tetraphenylethylene moieties as photosensitizers [56]. It was employed as photocatalyst for CDC reaction between *N*-aryl-THIQs and indole as nucleophilic coupling partner. Applying the same strategy, they also described the synthesis of **UiO-68Se**, which contains benzoselenadiazole units [58]. In this case, the nucleophile chosen was nitromethane, which was employed also as solvent. In 2019, He, Zhao and coworkers reported the synthesis of **Cu-TPA** MOF, which contains triphenylamine moieties as photosensitizers [52]. **Cu-TPA** presented moderated

photocatalytic activity on aza-Henry reaction, being possible to recycle it up to 3 times. In the same year, Duan and collaborators presented **ZJU-56** MOF [33] (Figure 15). It was constructed by mixing  $Zn^{II}$  salts with dicarboxylic linkers containing different ratios of pyridine and hydroxypyridinium salts. Because of its cationic and *N*-atom rich structure, it resulted on a two-photon responsive MOF, which was employed as an efficient photocatalyst in the aza-Henry reaction, using nitromethane as nucleophile and solvent, and several *N*-aryl-THIQs with different substituents in the phenyl ring. Finally, very recently, Li Zhang and collaborators [109] reported the synthesis of two porphyrin-containing MOFs, **Rh**- and **Ir**-PCN224, and their application as photocatalysts for the construction of C-P bonds between *N*-aryl-THIQs and different phosphites through CDC reactions.

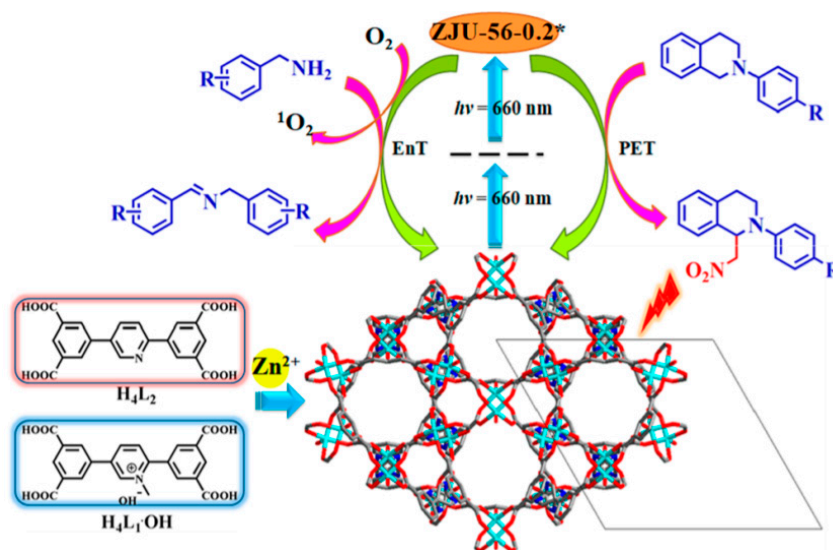


**Figure 15.** Construction of **ZJU-56** for two-photon absorption processes, containing pyridine and hydroxypyridinium fragments. Adapted with permission from Reference [33], Copyright (2019) American Chemical Society.

The functionalization strategy has also been applied in obtaining MOFs with photocatalytic activity for CDC reactions. Thus, a BODIPY photosensitizer was anchored to **UiO-68** through pending amino groups present in the linkers [69]. The **UiO-68-BP** was employed as heterogeneous photocatalyst for CDC reactions among different *N*-aryl-THIQs and different nitroalkanes. The same strategy was later employed by Khan and collaborators [70], who anchored the organic photocatalyst Eosin Y into **UiO-66-NH<sub>2</sub>** through amide bonds. The **EY@UiO-66-NH<sub>2</sub>** MOF was employed as photocatalyst in CDC reactions among different tertiary amines (not only THIQs) and various nucleophiles such as nitriles, phosphites, naphtols, malonates, and ketones.

**Table 12.** Photocatalytic CDC reaction mediated by MOFs.

Reactants	MOF	Strategy	Light	Power (W) <sup>1</sup>	Reference
<i>N</i> -arylTHIQ/nitromethane	UiO-67-doped	Pristine	White	26	[59]
<i>N</i> -arylTHIQ/acetone	UNLPP-12	Pristine	White	14	[32]
<i>N</i> -arylTHIQ/indol	UiO-68-mtpdc	Pristine	Blue LEDs	-	[56]
<i>N</i> -arylTHIQ/nitromethane	UiO-68Se	Pristine	Blue LEDs	-	[58]
<i>N</i> -arylTHIQ/nitromethane	Cu-TPA	Pristine	White	26	[52]
<i>N</i> -arylTHIQ/nitromethane	ZJU-56	Pristine	660 nm	13	[33]
<i>N</i> -arylTHIQ/phosphites	Ir-PCN-224	Pristine	>420 nm	-	[109]
<i>N</i> -arylTHIQ/nitroalkanes	UiO-68-BP	Functionalization	Green LEDs	-	[69]
Tertiary amines/various nucleophiles	EY@UiO-66-NH2	Functionalization	Visible	16	[70]

<sup>1</sup> Hyphen indicates that this value was not found in the original report.

*Cross-dehydrogenative coupling reactions mediated by COFs* (Table 13): In the field of COFs, this reaction has been scarcely explored. The two first examples of COFs as photocatalytic materials for organic transformations studied CDC as a proposed model reaction. Initially, at the end of 2016, Wu [27] employed a pristine acylhydrazone-based COF, **TFB-COF**, as photocatalyst for CDC reaction between different *N*-aryl-THIQs and various nucleophiles (i.e., ketones and nitro-derivatives). Almost at the same time, in 2017, Liu and collaborators [110] presented the applicability of **COF-JLU5**, an imine-based COF which contains triazine units, as heterogeneous photocatalyst in the same reaction, but with a wider scope of THIQs and nucleophiles (phosphite and malonates were added), and lower reaction times. Finally, two bidimensional imine-based COFs that contain triphenylamine and tetraphenylethylene units as photosensitizers were synthesized by Cui and coworkers [67]. They presented high photoredox activity for debromination and CDC reactions. Specifically, the CDC reaction between different *N*-aryl-THIQs and nitromethane as a coupling partner was efficiently catalyzed by both COFs.

**Table 13.** Photocatalytic CDC reaction mediated by COFs.

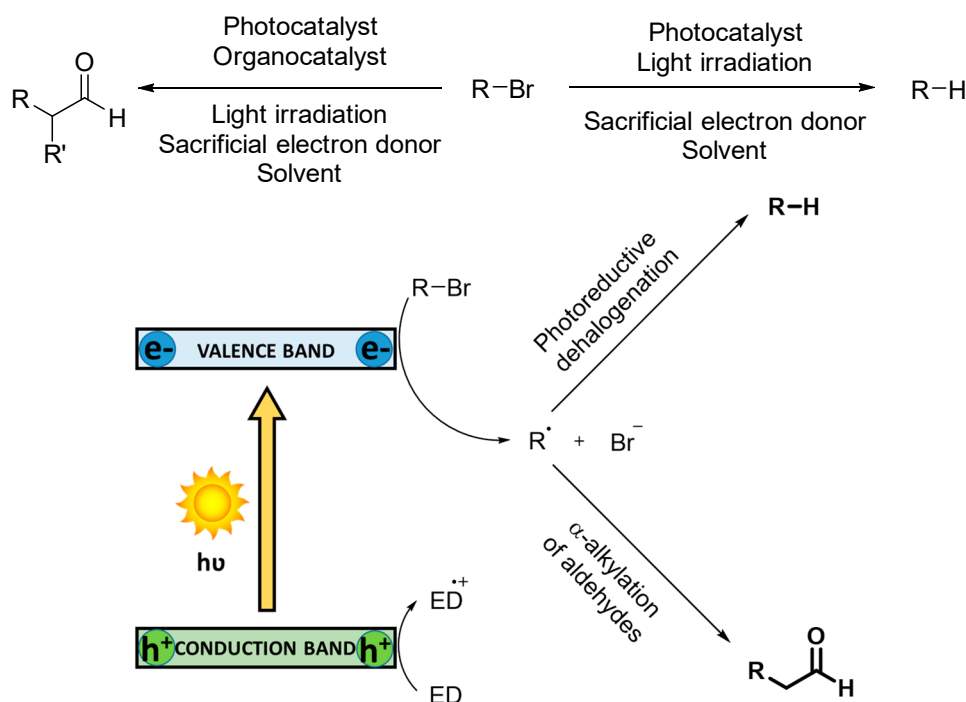
Reactants	COF (Linkage)	Strategy	Light	Power (W) <sup>1</sup>	Reference
<i>N</i> -arylTHIQs/ketones and nitro derivatives	TFB-COF (hydrazone-based)	Pristine (undecorated)	White	45	[27]
<i>N</i> -arylTHIQs/ketones, phosphites, malonates and nitro derivatives	COF-JLU-5 (imine-based)	Pristine (photoactive building block)	460 nm LEDs	30	[110]
<i>N</i> -arylTHIQs/nitromethane	COF-1, COF-2 (imine-based)	Pristine (photoactive building blocks)	White LEDs	-	[67]

<sup>1</sup> Hyphen indicates that this value was not found in the original report.

### 3.4. Dehalogenation

Organic halides are commonly used on organic synthesis because they are readily accessible and useful for obtaining different high-added value products. For instance, they can account for radical formation under light irradiation, resulting on C-C coupling of different nature. However, most brominated compounds are also considered as persistent pollutants. For example, polybrominated diphenylethers (PBDEs), which are frequently used as flame retardants in polymers and plastics, are demanded worldwide, but they are bioaccumulative and toxic [111]. Photocatalysis has emerged as a possible way to the remediation of this type of compounds through radical-involved reactions, such as photoreductive dehalogenation, where the halogen atom is substituted by a hydrogen atom [112]. Another method consists on the  $\alpha$ -alkylation of aldehydes where the formed radical is trapped by an enamine intermediate which after the catalytic cycle and hydrolysis allows the formation of the alkylated product. [113]. In both cases, a reductive quenching of the excited state of the photocatalyst

by the organic halide is observed, that allows the formation of the desired radical (Scheme 11). This radical will capture a hydrogen atom from the reaction medium (in the case of the photoreductive dehalogenation) or will be trapped by a strong electrophile such as an iminium ion (in the case of the alkylation of aldehydes).



**Scheme 11.** Generally accepted mechanism of dehalogenation reactions.

*Dehalogenation reactions mediated by MOFs* (Table 14): The most recurrent strategies in the construction of MOFs for dehalogenation processes consist not only on the design of photoactive linkers or clusters, but also on the functionalization and immobilization of organic and inorganic dyes through different interactions. The first example of dehalogenation in the field of MOFs was reported by Duan and coworkers in 2012, where **Zn-PYI1** and **Zn-PYI2** (enantiomers) were synthesized through the combination of a triphenylamine linker (the photosensitizer) with a chiral anchored amino-organocatalyst and Zn as the metal source [114] (Figure 16). These two MOFs were employed as bifunctional organo-photocatalyst in the asymmetric  $\alpha$ -alkylation of aldehydes. As organic halide, diethylbromomalonate was employed, and it was combined with different aliphatic aldehydes in the presence of 2,6-lutidine as a base. Excellent enantiomeric excesses and yields were reached, being possible to isolate the two enantiomeric products by using one MOF or another. In addition, size-discrimination studies were performed.

**Table 14.** Photocatalytic dehalogenation reactions mediated by MOFs.

Reactants	MOF	Strategy	Light	Power (W) <sup>1</sup>	Reference
Bromomalonate	Zn-PYI1, Zn-PYI2	Pristine	White	26	[114]
Aryl halides	Zn-PDI	Pristine	455 nm LEDs	-	[57]
Phenacyl bromide	Rudcbpy-UiO-67	Pristine	Hg lamp	125	[115]
Phenacyl bromide	SubPc@MIL-101(Cr)-NH <sub>2</sub>	Functionalization	Simulated sunlight	-	[71]
PBDE-209	NH <sub>2</sub> -MIL-125(Ti)	Pristine	Xe lamp, >420 nm	300	[116]

<sup>1</sup> Hyphen indicates that this value was not found in the original report.

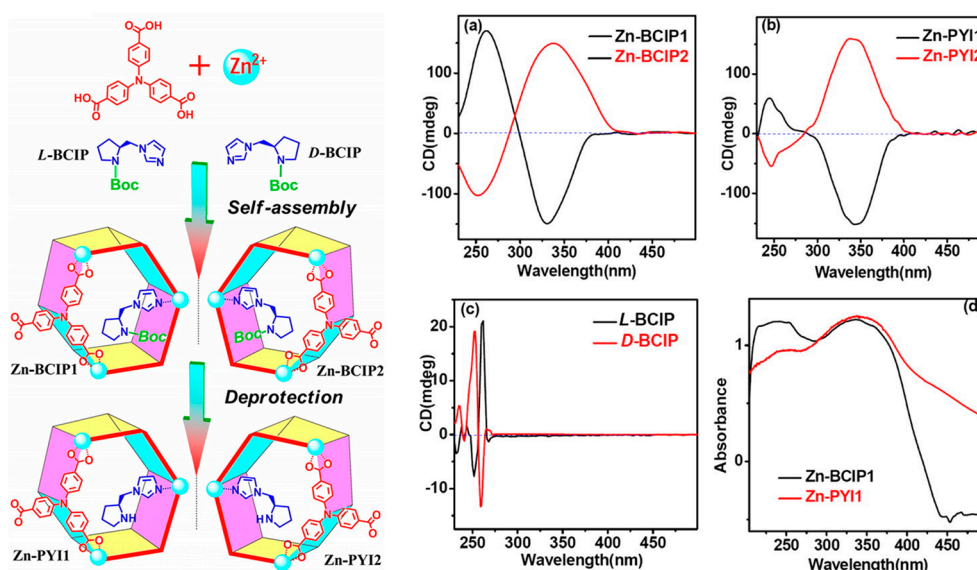


**Figure 16.** Synthesis and spectral characterization of chiral MOFs Zn-PYI1 and Zn-PYI2. Adapted with permission from Reference [114], Copyright (2012) American Chemical Society.

Later, in 2016, the same group reported the incorporation of perylene-diimide (PDI) as photosensitizing linker to afford **Zn-PDI** MOF [57]. This material was employed as heterogeneous photocatalyst in photoreductive dehalogenation processes, C–H aromatic substitution reactions, oxidation of benzylic alcohols and oxidative coupling of amines. In 2018, García and collaborators [115] reported the synthesis and spectroscopic properties of **Rudcbpy-UiO-67**, which contains Ru<sup>II</sup>-bipyridine moieties. This MOF was employed in the photoreductive debromination of phenacyl bromide. In 2019, the same group presented the anchorage of subphthalocyanines as photoredox units to **MIL-101(Cr)-NH<sub>2</sub>** through B–N interactions [71]. The **SubPc@MIL-101(Cr)-NH<sub>2</sub>** MOF was employed in the *in-situ* generation of phenacyl radical (from phenacyl bromide) coupled to the alkylation of styrene. Finally, very recently, Ma, Zhao, and coworkers [116] reported the application of **NH<sub>2</sub>-MIL-125(Ti)** as heterogeneous photocatalyst for the reductive debromination of decabromodiphenylether (PBDE-209) and studied the dependence of this reaction on the nature of the hole-scavenger employed. The best results were obtained when triethanolamine was used.

*Dehalogenation reactions mediated by COFs* (Table 15): In the field of COFs, three very recent contributions can be found in the literature. Two of them are devoted to the design of photoactive building blocks. On the one hand, Liu and collaborators [117] designed a benzothiadiazole–dialdehyde, able to condensate with a tetratopic-planar amine into a bidimensional imine-based COF, **JLU-22**. This COF was employed as photocatalyst for both photoreductive debromination and  $\alpha$ -alkylation of aldehydes, using different phenacyl bromides and bromomalonates as starting materials. On the



other hand, as previously explained in CDC section, two bidimensional imine-based COFs that contain triphenylamine and tetraphenylethylene units as photosensitizers were synthesized by Cui and coworkers [67] (Figure 17). They present high photoredox activity for debromination and CDC reactions. They performed the asymmetric  $\alpha$ -alkylation of aldehydes using a chiral imidazolidinone as organocatalyst and 2,6-lutidine as additive. As starting materials, different bromomalonates and sterically hindered aliphatic aldehydes were used, obtaining from moderate-to-good yields and excellent enantioselectivities. Finally, our group presented the covalent incorporation of photocatalytically active Pt<sup>II</sup>-hydroxyquinoline complexes into an imine-based layered COF through monomer truncation strategy. Pt@COF is able to act both as an energy transfer and electron transfer photocatalyst, presenting very high turnover numbers (>8000 TON) towards sulfoxidation and photoreductive dehalogenation reactions. In particular, different malonate, benzylic, phenacyl, and aromatic bromides were efficiently reduced to the corresponding products under mild and green conditions [72].

Table 15. Dehalogenation reactions mediated by COFs.

Reactants	COF (Linkage)	Strategy	Light	Power (W) <sup>1</sup>	Reference
Phenacyl bromides, bromomalonates	JLU-22 (imine-based)	Pristine (photoactive building block)	White LEDs	30	[117]
Bromomalonates	COF-1, COF-2 (imine-based)	Pristine (photoactive building block)	White LEDs	-	[67]
Malonate, benzylic, phenacyl and aromatic bromides	Pt@COF (imine-based)	Functionalization	450 nm LEDs	12	[72]

<sup>1</sup> Hyphen indicates that this value was not found in the original report.

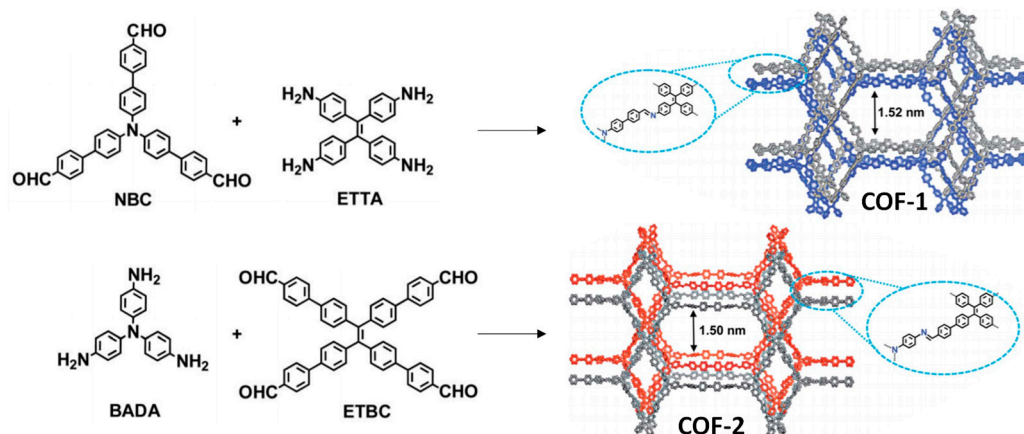


Figure 17. Synthesis of interpenetrated COF-1 and COF-2 as photoredox catalytic materials for dehalogenation reactions. Adapted from Reference [67], Published by the Royal Society of Chemistry.

### 3.5. Other Reactions

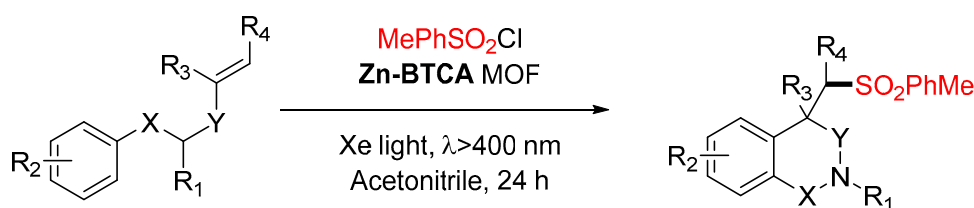
Apart from oxidation processes, oxidative couplings, cross-dehydrogenative couplings, and dehalogenation reactions, some other organic transformations have been tested in order to evaluate and probe the photocatalytic activity of MOFs and COFs.

In the field of MOFs (Table 16), the three strategies presented in Section 2 have been applied in different reactions. For example, in 2018, Duan and coworkers [49] designed different linkers containing triphenylamine and thiophene moieties in order to synthesize the pristine Zn-BTCA MOF. This MOF presented high photocatalytic activity in a sulfonylation–cyclization tandem reaction of *N*-arylmethacrylamides and *N*-aroxyl-methacrylamides (Scheme 12), leading to the formation of the corresponding arylsulfonyl isoquinolinediones or oxindoles.

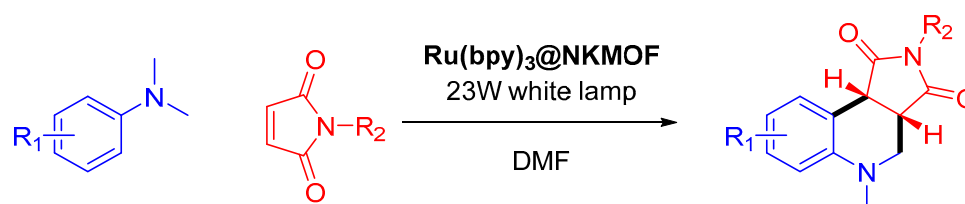
**Table 16.** Other photocatalytic organic transformations mediated by MOFs.

Reaction	MOF	Strategy	Light	Power (W) <sup>1</sup>	Reference
Sulfonylation-cyclization	Zn-BTCA	Pristine	Xe, <400 nm	-	[49]
Nitrophenol reduction	[Zn <sub>3</sub> (OH) <sub>2</sub> (ADBE <sub>2</sub> ) <sub>2</sub> ]	Pristine	Visible	-	[46]
N-Cyclization	Ru(bpy) <sub>3</sub> @NKMOF	Functionalization	White	23	[34]
Trifluoroethylation	UiO-67-Ir	Functionalization	White	32	[118]
Passerini	Zr-MOF-FePC	Functionalization	Hg lamp	500	[119]
Alkylation of nitriles	DT-BPY	Hybrid	Xe lamp	500	[48]
Light-induced Suzuki	CuPd@NH <sub>2</sub> -UiO-66(Zr)	Hybrid	Xe lamp	300	[79]
Amine-alcohol condensation	PdAu@MIL-100(Fe)	Hybrid	Xe lamp 420–800 nm	300	[78]

<sup>1</sup> Hyphen indicates that this value was not found in the original report.

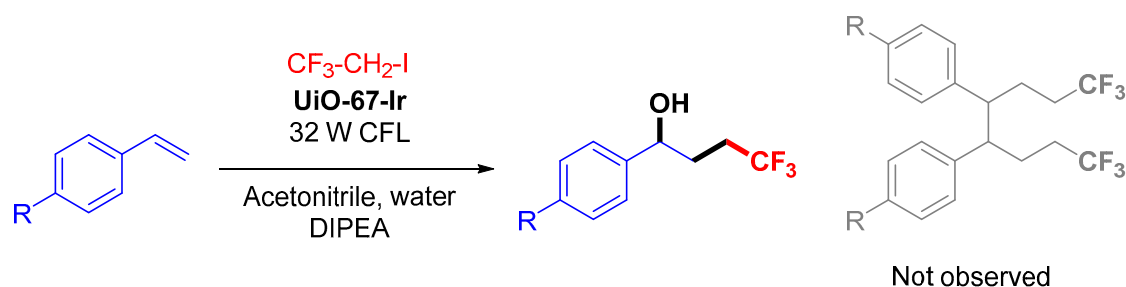
**Scheme 12.** Sulfonylation-cyclization tandem reaction mediated by Zn-BTCA MOF.

Another pristine photocatalytic MOF was obtained by Xing and collaborators [46], containing anthracene units. This material ([Zn<sub>3</sub>(OH)<sub>2</sub>(ADBE<sub>2</sub>)<sub>2</sub>]**·3DEF**) was capable of performing not only the synthesis of imine compounds through oxidative reactions, but also reductive processes, such as the reduction of nitrophenols to the corresponding anilines, using EtOH and hydrazine hydrate as solvents. In the same year, Cheng, Zhang, and coworkers [34] synthesize **Ru(bpy)<sub>3</sub>@NKMOFs** by an in situ construction of the corresponding ZIF in presence of Ru(bpy)<sub>3</sub>. The occluded complex was capable of catalyzing oxidation of organic bromides to the corresponding carbonylic compounds (see above), and also the cyclization reaction between tertiary anilines and maleimides, affording the synthesis of ring-fused tetrahydroquinolines (Scheme 13).

**Scheme 13.** Photocyclization reaction between tertiary anilines and maleimides.

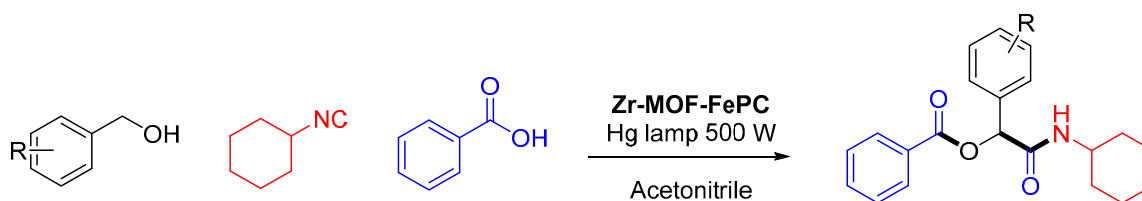
Post-functionalized MOFs played a key role in some examples of photocatalyzed organic transformations. In 2016, **UiO-67** was post-functionalized with two organometallic Ir complexes by Cohen and Yu [118]. The two **UiO-67-Ir** MOFs were tested in the trifluoroethylation of styrene, observing a change of selectivity from the homogeneously catalyzed reaction to the heterogeneous version (Scheme 14). When Ir-phenylpyridine homogenous complexes were tested, although full conversion was obtained, the major product was a dimeric species. However, when the complexes were immobilized and isolated into the porous framework, the reaction proceeded towards the mono-hydroxy-trifluoroethylated product. In addition, this change of selectivity was observed for 5 different substrates.





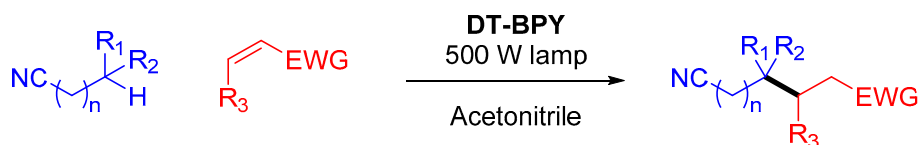
**Scheme 14.** Photocatalytic trifluoroethylation of styrene-derivatives by UiO-67-Ir MOFs.

On the other hand, in 2018, Azarifar and collaborators [119] carried out a post-synthetic modification of **UiO-66-NH<sub>2</sub>** with pyridinecarbaldehyde in order to chelate Fe(III) centers. The obtained **Zr-MOF-FePC** presented high photocatalytic activity in the multicomponent Passerini reaction (Scheme 15), leading to the isolation of  $\alpha$ -acyloxyamides by using a high power 500 W lamp as light source.



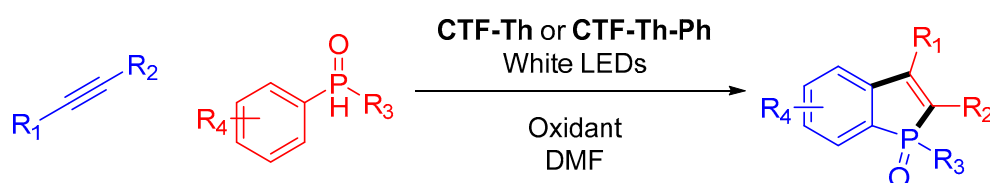
**Scheme 15.** Passerini reaction catalyzed by Zr-MOF-FePC.

Finally, some examples of hybrid MOFs can be found. For example, Duan and collaborators [48] synthesized the hybrid **DT-BPY**, which is formed by the combination of a photoactive decatungstate and a Cu-MOF, in order to perform the selective C-H alkylation of aliphatic nitriles under a high-power lamp (Scheme 16). In 2018, Li and coworkers [79] impregnated **NH<sub>2</sub>-UiO-66(Zr)** with Pd and Cu centers, that became Cu-Pd nanoclusters after a reductive treatment with NaBH<sub>4</sub>. The resulting hybrid **CuPd@NH<sub>2</sub>-UiO-66(Zr)** presented high photocatalytic activity and selectivity in light-induced Suzuki cross-coupling reactions between aryl iodides and arylboronic acids, avoiding homocoupling unproductive pathways. The same group applied the mentioned strategy in obtaining **PdAu@MIL-100(Fe)**, that is photocatalytically active in the tandem *N*-alkylation of amines with alcohols [78].



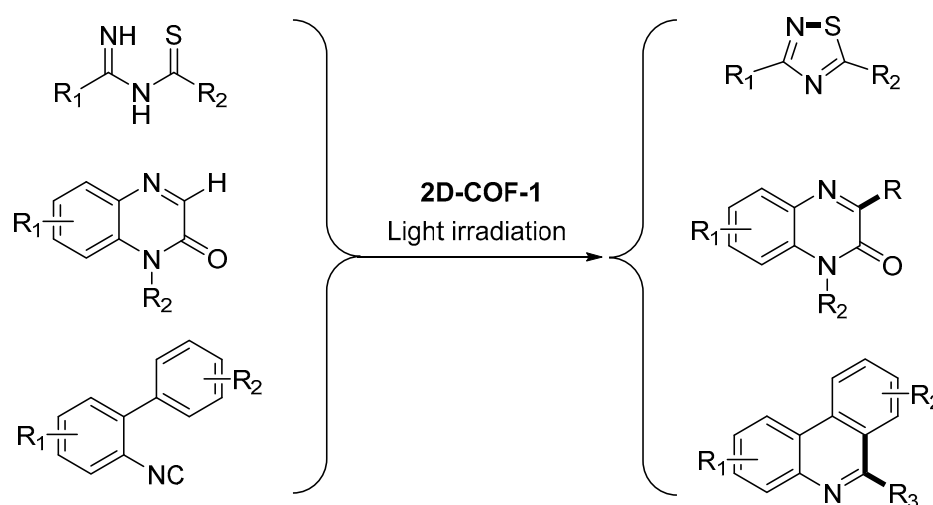
**Scheme 16.** Alkylation of nitriles.

In the field of COFs (Table 17), many contributions in other organic transformations can be found, related to the employ of pristine materials. The first example where COFs were used as photocatalysts is from 2016, when Zhang and collaborators [120] designed a CTF containing benzothiadiazole moieties through cyclotrimerization of nitriles, using SiO<sub>2</sub>-NPs as template for the material growth. This nanostructured CTF was employed as catalyst in the photoreduction of nitrophenol to aminophenol under green conditions. Two asymmetric CTFs were synthesized in 2018 by the same group, containing thiophene units. **CTF-Th** and **CTF-Th-Ph** were used for the photocatalytic synthesis of benzophosphole oxides, in presence of an external oxidant (Scheme 17) [121].



**Scheme 17.** Photocatalytic synthesis of benzophosphole oxides mediated by CTF-Th/CTF-Th-Ph.

In 2019 and 2020, Yang's group [122–124] employed **2D-COF-1**, an acylhydrazone-based COF, as photocatalytic pristine material in three different organic transformations: radical addition-cyclization of 2-arylphenylisocyanides [122], C3-arylation of quinoxalinones [123] and synthesis of 1,2,4-thiadiazoles [124] (Scheme 18). In the three cases, the catalyst was recycled up to 5 times without losing its photocatalytic activity under environmentally friendly conditions.



**Scheme 18.** Photocatalytic organic transformations mediated by **2D-COF-1**.

In 2019, an interesting application of a pristine  $\beta$ -ketoenamine-based COF (**TpTt**) for the photoisomerization of double C-C bonds was reported by Banerjee and collaborators [25]. The **TpTt-COF**, formed by the condensation of the readily accessible melamine and trimethylphloroglucinol, was employed in order to isomerize a variety of substituted olefins from *trans* to *cis* configuration under visible light irradiation. Parallely, Thomas and coworkers constructed donor-acceptor imine-based COFs containing triazine and thiophene/dithiophene units (**TTT-DTDA** and **TTT-BTDA**) as heterogeneous photosensitizers for radical polymerization processes under visible light irradiation [125]. Very recently, Li, Zhao and collaborators synthesized fully conjugated COFs through post-thermal treatment of imine-based COFs containing thiophene moieties. These materials were employed for the photoregeneration of NADH under visible light irradiation [24].

Apart from pristine COFs, only one example of hybrid material has been studied for other photocatalytic organic transformations by Kim and collaborators in 2018 [126]. In this work, they constructed **COF-LZU-1** (an imine-based COF) over **TiATA-MOF** (which contains amino moieties), and then a Pd source was added to the hybrid. After the reduction of Pd centers, the multicomponent material **Pd/TiATA@LZU1** was used for the selective photoreduction of styrene under visible light irradiation. The catalyst was recycled up to 8 times without losing its photocatalytic activity.

**Table 17.** Other photocatalytic organic transformations mediated by COFs.

Reaction	COF (Linkage)	Strategy	Light	Power (W) <sup>1</sup>	Reference
Nitrophenol reduction	CTF-BT, CTF-B (triazines)	Pristine (photoactive linkage)	White LEDs	12	[120]
Benzophosphole oxides synthesis	CTF-Th, CTF-Th-Ph (triazines)	Pristine (photoactive linkage)	White LEDs	-	[121]
Radical addition + cyclization	2D-COF-1 (hydrazone-based)	Pristine (undecorated)	Blue LEDs	34	[122]
C3-arylation of quinoxalinones	2D-COF-1 (hydrazone-based)	Pristine (undecorated)	Blue LEDs	34	[123]
Synthesis of 1,2,4-thiadiazoles	2D-COF-1 (hydrazone-based)	Pristine (undecorated)	Blue LEDs	34	[124]
Olefins isomerization	TpTt (B-ketoenamine-based)	Pristine (photoactive building block, triazine)	Blue LEDs	34	[25]
Radical polymerization	TTT-DTDA/TTT-BTDA (imine-based)	Pristine (photoactive building block, triazine)	Xe lamp, <420 nm	300	[125]
NADH regeneration	Fully conjugated COFs	Pristine	Xe lamp, <420 nm	300	[24]
Styrene reduction	Pd/TiATA@LZU1	Hybrid	Xe lamp, <420 nm	300	[126]

<sup>1</sup> Hyphen indicates that this value was not found in the original report.

#### 4. Comparative Critical Discussion on the Use of MOFs and COFs in Photocatalytic Organic Transformations

Up to this point, all available data in literature reporting the use of MOFs and COFs on photocatalytic organic transformations have been systematically presented in this review. This last section is intended to offer a brief comparative overview about the inherent features of one and another family of materials.

A detailed analysis of the presented examples revealed different tendencies on the use of both MOFs and COFs. First, it is worth to mention that the first report where MOFs were synthesized and characterized was published in 1999 [1]. Few years later, the first COF was published in 2005 [2]. Even though COFs have been object of study for fifteen years now, the quantity of works devoted to this family of materials is significantly lower than the studies invested in the use of MOFs. Although the time span between the invention of MOFs and the discovery of COFs could be one reason for the different attention that attracted both kind of materials, also it should be taken into account that crystalline MOFs (even single crystals) are easier to obtain. Therefore, the feasibility of structural insights on MOFs boosted the exploration of many applications of these materials. Consequently, applications of COFs are still underrepresented in the current literature in comparison with their metal–organic analogues. In particular, some distinct strategies have been used in the design of both photocatalytically active MOFs and COFs. While pristine MOFs represent the 60% of examples of photocatalytic synthetic applications, for COFs, this contribution reaches 90%. In addition, they differ in the applied sub-strategy (see Section 2.1 for further details): as far as MOFs are concerned, the design of intrinsically photoactive linkers is the dominant procedure, while for COFs, the use of imine-,  $\beta$ -ketoenamine-, hydrazone- or cyanovinylene-based undecorated materials is preferred. This difference can be attributed to the enhanced electronic delocalization that occurs in highly conjugated COFs but resulting difficult on MOFs, because of the presence of metal centers in a variety of coordination environments. Thus, the difficult conjugation and electron delocalization observed for MOFs, make necessary the predesign and introduction of photoactive linkers into the material backbone. Otherwise, functionalization protocols or obtaining hybrid photoactive materials have been extensively studied in MOFs but remains scarcely explored for COFs. In fact, the major part of examples found for functionalized or hybrid COFs are devoted to HER or carbon dioxide photoreduction, which are not part of this review [18]. In contrast, although some examples of MOF-hybrid materials are also applied

to HER [127] and CO<sub>2</sub> photoreduction [128], many examples of photocatalytic applications of such kind of materials can be found. Among them, the selective oxidation of aromatic alcohols is the one that attracted more attention.

In this review, we considered four main photocatalytic organic transformations: oxidation, oxidative coupling, cross-dehydrogenative coupling, and dehalogenation reactions. These reactions imply that 85% of all the photocatalytic organic transformations are mediated by MOFs. However, this group of transformations only represent 70% of the photocatalytic organic processes catalyzed by COFs. This observation is suggesting that COFs seem to be more versatile as photocatalytic platforms for organic transformations. It can be attributed to the possibility of design and modulation of the photophysical properties of organic frameworks.

In this review, catalytic materials have been classified into three different synthetic strategies: pristine, functionalized, and hybrid materials. Each of them has its advantages and disadvantages. For example, the use of pristine materials requires a careful design of the building blocks taking into account length and orientations. In contrast, pristine materials have generally the advantage of obtaining homogeneous materials, being the porosity and pore size easily controllable. On the other hand, post-functionalized materials generally do not require such an exhaustive design of the building blocks, allowing easier synthetic procedures. However, the post-functionalization process makes it difficult to control the following factors: (1) the catalytic loading, (2) the homogeneity of the material, and (3) the porosity and pore size. Finally, hybrid materials make possible the combination of very diverse properties, which gives rise to synergistic phenomena. However, it is difficult to find the appropriate strategy to avoid the segregation of the different components. Furthermore, the interaction at the interfaces does not always allow interplay between materials of different nature.

*Light source:* Another important subject to discuss is the different type of employed light source. In photochemistry, light is crucial, since it brings with it the essential energy to excite the photocatalyst into its excited state, generating the corresponding charge separation. Thus, it is mandatory to control the power of the light source, as well as its energy. On the one hand, high-power lamps can lead to decomposition processes, such as photobleaching of the material [129]. On the other hand, the use of high energy sources (UV lamps) can lead to background or side reactions. These factors must be considered, taking into account that several examples presented in this review use high energy or high-power light sources, which can account for undesired side reactions or uncatalyzed background pathways. For example, results found in our laboratory demonstrated that in dehalogenation reactions high power and/or UV lamps can lead to the scission of C–Br or C–I bonds in the absence of photocatalyst. Therefore, background processes should always be considered and substrates that do not show background pathways (under specific reaction conditions) must be employed. In addition, it is important to adequate the wavelength of the employed radiation to the band gap of the corresponding heterogeneous photocatalyst, in order to maximize the photon transfer and to minimize the loss of energy [17]. In such a way, the use of visible light LEDs seems to be the best option, since they allow the exhaustive control over the wavelength and they present low power energy [62,72]. The design of materials with two-photon absorption capability results are quite interesting, inasmuch as low energies (such as red light or even infrared irradiation) are useful for these type of systems [28,33]. As an alternative, the use of UV-Visible Xe or Hg lamps equipped with cut-off filters frequently appears in some of the examples presented herein [75]. However, the major part of the energy of these irradiation systems is lost in the filter, so the overall conversion of light energy into the chemical transformation is scarce. Therefore, sunlight or more efficient LEDs should be used in future studies.

*Catalyst loading:* Catalyst loading or reaction scale are parameters that widely change from one example to another of those presented in this review. The different conditions found in the literature can account for different factors, such as the dispersibility of the material, the opacity of the system, the concentration of the solution or the nature of the light source. It is evident that low catalyst loadings are desired, since they allow to obtain high turnover numbers, and the opacity of the system is significantly decreased, which oppositely increase the efficiency of the photon absorption by the

photocatalyst. In some reported cases, the catalyst loading implies the use of similar weights of photocatalytic material and reagents. Even though this does not seem to be an economically efficient strategy, the ratio between the moles of substrates transformed and the number of catalytically active sites is not obvious. This is because in many cases not all the material is equally active, being the surface the main responsible of the photocatalytic activity. Otherwise, scalability of heterogeneous photochemistry is quite difficult. In all the related examples, the scale is maintained below to 3 mmol scale [78], which is far from the requirements of fine chemicals industry. Resorting to flow photochemistry is therefore a remaining challenge on this field.

*Solvent:* The election of the solvent can also drastically change the catalytic outcome of the photocatalyzed reactions and their further applications. This is because some factors, such as suspension and stability of the heterogeneous photocatalyst, the solubility of the reagents and products and the photophysical properties of the solvated catalyst and substrates, can have a significant effect on the photocatalytic outcome. In addition, non-toxic solvents such as water are the most desired ones, which could fulfill the requirements of green chemistry. However, not all heterogeneous catalysts are stable enough against hydrolysis processes. For example, a variety of MOFs and boroxine- or boronate-based COFs are readily disassembled in aqueous media, limiting their applications. Thus, some strategies have been developed in order to obtain hydrolysis-stable MOFs, such as the use of high-valent metal-containing MOFs with O-enriched linkers or low-valent metal-containing MOFs with N-enriched linkers, as well as the employ of hydrophobic ligands or post-synthetic modification protocols [130]. Otherwise, the development of different hydrolysis-stable types of linkages (see Section 2 for further details) was the key on the field of COFs. Due to the characteristics of MOF and COFs systems, in most cases polar organic solvents such as acetonitrile, aliphatic alcohols or ethers are employed.

*Stability/Integrity:* A final factor that should be taken into account regarding the stability of photocatalytic materials is the possible chemical erosion triggered by its reactivity with the organic substrates. In particular, it has been observed that imine-based COFs are sensitive to nucleophilic attack of reagents, such as amines or malononitriles, as a consequence of the reversible nature of the imine bond [107]. This decomposition can compete with catalyzed reactions, that uses this kind of reagents (e.g., oxidative coupling of amines). Therefore, leaching and recyclability experiments should be performed in order to discard the disassembly of the material under the specific reaction conditions.

## 5. Concluding Remarks and Perspectives

The extensive overview of the available literature devoted to organic synthetic applications of photocatalytic systems based on COFs and MOFs demonstrates the versatility of these materials and their potential for further findings. From a structural point of view, strategies for the design of reticular materials, with a variety of geometries and topologies, has reached a high degree of maturity. As a consequence, some of the most common photocatalytic transformations reported for molecular systems have already been reported for reticular materials, and this review has carefully compiled the recent literature in this respect. However, considering the volume of work published and the complexity of processes and products reported, it seems that this field is still in its infancy. In fact, the MOFs/COFs scientific community has a clear bias towards the detailed structural elucidation and physical characterization of such reticular materials. However, the study of their catalytic (and in particular photocatalytic) applications are still very limited. As a consequence, apart from punctual cases, the typical mentioned transformations are currently studied as model systems, without exploring the full catalytic potential of many MOFs and COFs. Many challenges addressed on molecular systems remain clearly underexplored for photocatalytic MOFs or COFs, such as synthesis of asymmetric products or cooperative multicomponent catalysis. In addition, the particular advantages that could be specifically derived from the use of reticular materials have not been fully explored. In this sense, the examples of size discrimination phenomena or confinement effects are underrepresented in literature. Thus, further significant developments could be related to these aspects.



Interestingly, a comparable number of works have been found using MOFs and COFs for photocatalytic organic synthetic applications. This fact is somehow surprising considering that the number of MOFs reported is approximately two orders of magnitude higher than the number of COFs. Further work will be needed to determine if this observation is related to the different intrinsic nature of both kind of materials or is just the result of the different focus that the MOF and COF communities apply to their research. However, it is worth to note that the wide range of possibilities that COFs offer for the incorporation of predesigned organic fragments makes this kind of materials especially appealing for advanced photocatalytic applications.

From a methodological perspective, the examination of the literature available should serve to establish some principles that would allow to ensure the significance of the results and the future benchmarking of the published data. Up to now, a series of factors have not been systematically considered, making difficult the comparison between different systems. Some of these factors are wavelength and power of light source, checking of uncatalyzed photochemical background reactions, evaluation of recyclability and leaching phenomena, or the relative catalytic loading (which in some cases is stoichiometric or even superstoichiometric). Systematic incorporation of discussions on these factors in future works would be extremely useful.

Overall, the body of data compiled in this review confirms that the state of the art of photocatalytic applications of COFs and MOFs for organic transformations allows the laying of foundations of future developments. Therefore, much research is expected in the next few years that could fully explore all the potential of reticular chemistry to address the challenges that modern chemistry has ahead in the fields of energy conversion, design of environmentally benign processes or the production of high added value products.

**Author Contributions:** Conceptualization, A.L.-M., A.J.-A., J.A. and R.M.-B.; Data curation and draft preparation, A.L.-M. and A.J.-A.; Writing—review and editing, A.L.-M., A.J.-A., J.A. and R.M.-B.; supervision and Funding Acquisition J.A. and R.M.-B.; All authors have read and agreed to the published version of the manuscript.

**Funding:** Financial support was provided by the European Research Council (ERC-CoG, contract number: 647550), Spanish Government (PID2019-110637RB-I00, RTI2018-095038-B-I00), “Comunidad de Madrid” and European Structural Funds (S2018/NMT-4367).

**Conflicts of Interest:** The authors declare no conflict of interest. The funders had no role in the design of the study; in the collection, analyses, or interpretation of data; in the writing of the manuscript, or in the decision to publish the results.

## Abbreviations

For uncommon abbreviations outlined throughout the manuscript, see the following list: metal–organic frameworks—MOFs, covalent organic frameworks—COFs, secondary building units—SBUs, zeolitic imidazolate frameworks—ZIFs, covalent triazine frameworks—CTFs, hydrogen evolution reaction—HER, borondipyrromethene—BODIPY, nanoparticles—NPs, localized surface plasmon resonance—LSPR, bismuth ferrite—BFO, 1,4-diazabicyclooctane—DABCO, turnover number—TON, (2,2,6,6-Tetramethylpiperidin-1-yl)oxyl or (2,2,6,6-tetramethylpiperidin-1-yl)oxidanyl—TEMPO, light emitting diode—LED, cross dehydrogenative coupling—CDC, tetrahydroisoquinoline—THIQ, polybrominated diphenyl ether—PBDE, nicotine adenine dinucleotide—NADH, ultraviolet—UV.

## References

1. Li, H.; Eddaoudi, M.; O’Keeffe, M.; Yaghi, O.M. Design and synthesis of an exceptionally stable and highly porous metal-organic framework. *Nature* **1999**, *402*, 276–279. [[CrossRef](#)]
2. Côté, A.P.; Benin, A.I.; Ockwig, N.W.; O’Keeffe, M.; Matzger, A.J.; Yaghi, O.M. Porous, Crystalline, Covalent Organic Frameworks. *Science* **2005**, *310*, 1166–1170. [[CrossRef](#)] [[PubMed](#)]
3. Yaghi, O.M. Reticular Chemistry in All Dimensions. *ACS Cent. Sci.* **2019**, *5*, 1295–1300. [[CrossRef](#)] [[PubMed](#)]
4. Furukawa, H.; Cordova, K.E.; O’Keeffe, M.; Yaghi, O.M. The Chemistry and Applications of Metal-Organic Frameworks. *Science* **2013**, *341*, 1230444. [[CrossRef](#)] [[PubMed](#)]
5. Baumann, A.E.; Burns, D.A.; Liu, B.; Thoi, V.S. Metal-organic framework functionalization and design strategies for advanced electrochemical energy storage devices. *Commun. Chem.* **2019**, *2*, 86. [[CrossRef](#)]



6. Soni, S.; Bajpai, P.K.; Arora, C. A review on metal-organic framework: Synthesis, properties and application. *Charact. Appl. Nanomater.* **2018**, *2*. [[CrossRef](#)]
7. Segura, J.L.; Royuela, S.; Mar Ramos, M. Post-synthetic modification of covalent organic frameworks. *Chem. Soc. Rev.* **2019**, *48*, 3903–3945. [[CrossRef](#)]
8. Ding, S.-Y.; Wang, W. Covalent organic frameworks (COFs): From design to applications. *Chem. Soc. Rev.* **2013**, *42*, 548–568. [[CrossRef](#)]
9. Sharma, R.K.; Yadav, P.; Yadav, M.; Gupta, R.; Rana, P.; Srivastava, A.; Zbořil, R.; Varma, R.S.; Antonietti, M.; Gawande, M.B. Recent development of covalent organic frameworks (COFs): Synthesis and catalytic (organic-electro-photo) applications. *Mater. Horiz.* **2020**, *7*, 411–454. [[CrossRef](#)]
10. Lohse, M.S.; Bein, T. Covalent Organic Frameworks: Covalent Organic Frameworks: Structures, Synthesis, and Applications. *Adv. Funct. Mater.* **2018**, *28*, 1870229. [[CrossRef](#)]
11. Guo, Z.; Liu, B.; Zhang, Q.; Deng, W.; Wang, Y.; Yang, Y. Recent advances in heterogeneous selective oxidation catalysis for sustainable chemistry. *Chem. Soc. Rev.* **2014**, *43*, 3480–3524. [[CrossRef](#)] [[PubMed](#)]
12. Xu, C.; Ravi Anusuyadevi, P.; Aymonier, C.; Luque, R.; Marre, S. Nanostructured materials for photocatalysis. *Chem. Soc. Rev.* **2019**, *48*, 3868–3902. [[CrossRef](#)] [[PubMed](#)]
13. Augugliaro, V.; Palmisano, G.; Palmisano, L.; Soria, J. *Chapter 1—Heterogeneous Photocatalysis and Catalysis: An Overview of Their Distinctive Features*; Elsevier: Netherlands, Amsterdam, 2019; pp. 1–24. ISBN 978-0-444-64015-4.
14. Fensterbank, L.; Goddard, J.-P.; Ollivier, C.; Prier, C.K.; MacMillan, D.W.C. Visible-Light-Mediated Free Radical Synthesis. In *Visible Light Photocatalysis in Organic Chemistry*; John Wiley & Sons: New York City, NY, USA, 2018; pp. 25–71.
15. Wang, X.; Anpo, M.; Fu, X. (Eds.) *1—Introduction*; Elsevier: Netherlands, Amsterdam, 2020; pp. 1–6. ISBN 978-0-12-819000-5.
16. Shaw, M.H.; Twilton, J.; MacMillan, D.W.C. Photoredox Catalysis in Organic Chemistry. *J. Org. Chem.* **2016**, *81*, 6898–6926. [[CrossRef](#)] [[PubMed](#)]
17. Cui, Y.; Zhang, J.; He, H.; Qian, G. Photonic functional metal-organic frameworks. *Chem. Soc. Rev.* **2018**, *47*, 5740–5785. [[CrossRef](#)]
18. Wang, G.-B.; Li, S.; Yan, C.-X.; Zhu, F.-C.; Lin, Q.-Q.; Xie, K.-H.; Geng, Y.; Dong, Y.-B. Covalent organic frameworks: Emerging high-performance platforms for efficient photocatalytic applications. *J. Mater. Chem. A* **2020**, *8*, 6957–6983. [[CrossRef](#)]
19. Samanta, P.; Desai, A.V.; Let, S.; Ghosh, S.K. Advanced Porous Materials for Sensing, Capture and Detoxification of Organic Pollutants toward Water Remediation. *ACS Sustain. Chem. Eng.* **2019**, *7*, 7456–7478. [[CrossRef](#)]
20. Dhakshinamoorthy, A.; Li, Z.; Garcia, H. Catalysis and photocatalysis by metal organic frameworks. *Chem. Soc. Rev.* **2018**, *47*, 8134–8172. [[CrossRef](#)]
21. Chen, B.; Yang, Z.; Zhu, Y.; Xia, Y. Zeolitic imidazolate framework materials: Recent progress in synthesis and applications. *J. Mater. Chem. A* **2014**, *2*, 16811–16831. [[CrossRef](#)]
22. Uribe-Romo, F.J.; Hunt, J.R.; Furukawa, H.; Klöck, C.; O’Keeffe, M.; Yaghi, O.M. A Crystalline Imine-Linked 3-D Porous Covalent Organic Framework. *J. Am. Chem. Soc.* **2009**, *131*, 4570–4571. [[CrossRef](#)]
23. Waller, P.J.; Lyle, S.J.; Osborn Popp, T.M.; Diercks, C.S.; Reimer, J.A.; Yaghi, O.M. Chemical Conversion of Linkages in Covalent Organic Frameworks. *J. Am. Chem. Soc.* **2016**, *138*, 15519–15522. [[CrossRef](#)]
24. Wang, Y.; Liu, H.; Pan, Q.; Wu, C.; Hao, W.; Xu, J.; Chen, R.; Liu, J.; Li, Z.; Zhao, Y. Construction of Fully Conjugated Covalent Organic Frameworks via Facile Linkage Conversion for Efficient Photoenzymatic Catalysis. *J. Am. Chem. Soc.* **2020**, *142*, 5958–5963. [[CrossRef](#)] [[PubMed](#)]
25. Bhadra, M.; Kandambeth, S.; Sahoo, M.K.; Addicoat, M.; Balaraman, E.; Banerjee, R. Triazine Functionalized Porous Covalent Organic Framework for Photo-organocatalytic E–Z Isomerization of Olefins. *J. Am. Chem. Soc.* **2019**, *141*, 6152–6156. [[CrossRef](#)] [[PubMed](#)]
26. Stegbauer, L.; Schwinghammer, K.; Lotsch, B. V A hydrazone-based covalent organic framework for photocatalytic hydrogen production. *Chem. Sci.* **2014**, *5*, 2789–2793. [[CrossRef](#)]
27. Liu, W.; Su, Q.; Ju, P.; Guo, B.; Zhou, H.; Li, G.; Wu, Q. A Hydrazone-Based Covalent Organic Framework as an Efficient and Reusable Photocatalyst for the Cross-Dehydrogenative Coupling Reaction of N-Aryltetrahydroisoquinolines. *ChemSusChem* **2017**, *10*, 664–669. [[CrossRef](#)] [[PubMed](#)]

28. Shi, J.-L.; Chen, R.; Hao, H.; Wang, C.; Lang, X. 2D sp<sup>2</sup> Carbon-conjugated Porphyrin Covalent Organic Framework for Cooperative Photocatalysis with TEMPO. *Angew. Chem. Int. Ed.* **2020**, *59*, 9088. [[CrossRef](#)] [[PubMed](#)]
29. Xie, M.-H.; Yang, X.-L.; Zou, C.; Wu, C.-D. A Sn<sup>IV</sup>-Porphyrin-Based Metal-Organic Framework for the Selective Photo-Oxygenation of Phenol and Sulfides. *Inorg. Chem.* **2011**, *50*, 5318–5320. [[CrossRef](#)]
30. Feng, D.; Chung, W.-C.; Wei, Z.; Gu, Z.-Y.; Jiang, H.-L.; Chen, Y.-P.; Darensbourg, D.J.; Zhou, H.-C. Construction of Ultrastable Porphyrin Zr Metal-Organic Frameworks through Linker Elimination. *J. Am. Chem. Soc.* **2013**, *135*, 17105–17110. [[CrossRef](#)]
31. Johnson, J.A.; Zhang, X.; Reeson, T.C.; Chen, Y.-S.; Zhang, J. Facile Control of the Charge Density and Photocatalytic Activity of an Anionic Indium Porphyrin Framework via in Situ Metalation. *J. Am. Chem. Soc.* **2014**, *136*, 15881–15884. [[CrossRef](#)]
32. Johnson, J.A.; Luo, J.; Zhang, X.; Chen, Y.-S.; Morton, M.D.; Echeverría, E.; Torres, F.E.; Zhang, J. Porphyrin-Metalation-Mediated Tuning of Photoredox Catalytic Properties in Metal-Organic Frameworks. *ACS Catal.* **2015**, *5*, 5283–5291. [[CrossRef](#)]
33. Li, H.; Yang, Y.; He, C.; Zeng, L.; Duan, C. Mixed-Ligand Metal-Organic Framework for Two-Photon Responsive Photocatalytic C–N and C–C Coupling Reactions. *ACS Catal.* **2019**, *9*, 422–430. [[CrossRef](#)]
34. Yang, X.; Liang, T.; Sun, J.; Zaworotko, M.J.; Chen, Y.; Cheng, P.; Zhang, Z. Template-Directed Synthesis of Photocatalyst-Encapsulating Metal-Organic Frameworks with Boosted Photocatalytic Activity. *ACS Catal.* **2019**, *9*, 7486–7493. [[CrossRef](#)]
35. Wei, L.-Q.; Ye, B.-H. Cyclometalated Ir–Zr Metal-Organic Frameworks as Recyclable Visible-Light Photocatalysts for Sulfide Oxidation into Sulfoxide in Water. *ACS Appl. Mater. Interfaces* **2019**, *11*, 41448–41457. [[CrossRef](#)] [[PubMed](#)]
36. Wei, H.; Guo, Z.; Liang, X.; Chen, P.; Liu, H.; Xing, H. Selective Photooxidation of Amines and Sulfides Triggered by a Superoxide Radical Using a Novel Visible-Light-Responsive Metal-Organic Framework. *ACS Appl. Mater. Interfaces* **2019**, *11*, 3016–3023. [[CrossRef](#)] [[PubMed](#)]
37. Yuan, S.; Feng, L.; Wang, K.; Pang, J.; Bosch, M.; Lollar, C.; Sun, Y.; Qin, J.; Yang, X.; Zhang, P.; et al. Stable Metal-Organic Frameworks: Design, Synthesis, and Applications. *Adv. Mater.* **2018**, *30*, 1704303. [[CrossRef](#)] [[PubMed](#)]
38. Todorova, T.K.; Rozanska, X.; Gervais, C.; Legrand, A.; Ho, L.N.; Berruyer, P.; Lesage, A.; Emsley, L.; Farrusseng, D.; Canivet, J.; et al. Molecular Level Characterization of the Structure and Interactions in Peptide-Functionalized Metal-Organic Frameworks. *Chem.—Eur. J.* **2016**, *22*, 16531–16538. [[CrossRef](#)]
39. Feng, D.; Gu, Z.-Y.; Li, J.-R.; Jiang, H.-L.; Wei, Z.; Zhou, H.-C. Zirconium-Metalloporphyrin PCN-222: Mesoporous Metal-Organic Frameworks with Ultrahigh Stability as Biomimetic Catalysts. *Angew. Chem. Int. Ed.* **2012**, *51*, 10307–10310. [[CrossRef](#)]
40. Yu, J.; Cui, Y.; Wu, C.; Yang, Y.; Wang, Z.; O’Keeffe, M.; Chen, B.; Qian, G. Second-Order Nonlinear Optical Activity Induced by Ordered Dipolar Chromophores Confined in the Pores of an Anionic Metal-Organic Framework. *Angew. Chem. Int. Ed.* **2012**, *51*, 10542–10545. [[CrossRef](#)]
41. Devic, T.; Serre, C. High valence 3p and transition metal based MOFs. *Chem. Soc. Rev.* **2014**, *43*, 6097–6115. [[CrossRef](#)]
42. Wang, X.; Lu, W.; Gu, Z.-Y.; Wei, Z.; Zhou, H.-C. Topology-guided design of an anionic bor-network for photocatalytic [Ru(bpy)<sub>3</sub>]<sup>2+</sup> encapsulation. *Chem. Commun.* **2016**, *52*, 1926–1929. [[CrossRef](#)]
43. Wang, G.; Liu, Y.; Huang, B.; Qin, X.; Zhang, X.; Dai, Y. A novel metal-organic framework based on bismuth and trimesic acid: Synthesis, structure and properties. *Dalt. Trans.* **2015**, *44*, 16238–16241. [[CrossRef](#)]
44. Köppen, M.; Beyer, O.; Wuttke, S.; Lüning, U.; Stock, N. Synthesis, functionalisation and post-synthetic modification of bismuth metal-organic frameworks. *Dalt. Trans.* **2017**, *46*, 8658–8663. [[CrossRef](#)] [[PubMed](#)]
45. Bai, Y.; Dou, Y.; Xie, L.-H.; Rutledge, W.; Li, J.-R.; Zhou, H.-C. Zr-based metal-organic frameworks: Design, synthesis, structure, and applications. *Chem. Soc. Rev.* **2016**, *45*, 2327–2367. [[CrossRef](#)] [[PubMed](#)]
46. Chen, P.; Guo, Z.; Liu, X.; Lv, H.; Che, Y.; Bai, R.; Chi, Y.; Xing, H. A visible-light-responsive metal-organic framework for highly efficient and selective photocatalytic oxidation of amines and reduction of nitroaromatics. *J. Mater. Chem. A* **2019**, *7*, 27074–27080. [[CrossRef](#)]
47. Yu, X.; Wang, L.; Cohen, S.M. Photocatalytic metal-organic frameworks for organic transformations. *CrystEngComm* **2017**, *19*, 4126–4136. [[CrossRef](#)]

48. Shi, D.; He, C.; Sun, W.; Ming, Z.; Meng, C.; Duan, C. A photosensitizing decatungstate-based MOF as heterogeneous photocatalyst for the selective C–H alkylation of aliphatic nitriles. *Chem. Commun.* **2016**, *52*, 4714–4717. [[CrossRef](#)] [[PubMed](#)]
49. Zhang, T.; Shi, Y.; Zhang, S.; Jia, C.; He, C.; Duan, C. Thiophene insertion for continuous modulation of the photoelectronic properties of triphenylamine-based metal–organic frameworks for photocatalytic sulfonylation–cyclisation of activated alkenes. *New J. Chem.* **2018**, *42*, 18448–18457. [[CrossRef](#)]
50. Fujie, K.; Otsubo, K.; Ikeda, R.; Yamada, T.; Kitagawa, H. Low temperature ionic conductor: Ionic liquid incorporated within a metal–organic framework. *Chem. Sci.* **2015**, *6*, 4306–4310. [[CrossRef](#)]
51. Lin, W.; Hu, Q.; Jiang, K.; Yang, Y.; Yang, Y.; Cui, Y.; Qian, G. A porphyrin-based metal–organic framework as a pH-responsive drug carrier. *J. Solid State Chem.* **2016**, *237*, 307–312. [[CrossRef](#)]
52. Shi, D.; Guo, X.; Lai, T.; Zheng, K.; Wu, Q.; Sun, C.; He, C.; Zhao, J. A tetrazole-containing triphenylamine-based metal–organic framework: Synthesis and photocatalytic oxidative CC coupling reaction. *Inorg. Chem. Commun.* **2019**, *105*, 9–12. [[CrossRef](#)]
53. Dan-Hardi, M.; Serre, C.; Frot, T.; Rozes, L.; Maurin, G.; Sanchez, C.; Férey, G. A New Photoactive Crystalline Highly Porous Titanium(IV) Dicarboxylate. *J. Am. Chem. Soc.* **2009**, *131*, 10857–10859. [[CrossRef](#)]
54. Wang, D.; Wang, M.; Li, Z. Fe-Based Metal–Organic Frameworks for Highly Selective Photocatalytic Benzene Hydroxylation to Phenol. *ACS Catal.* **2015**, *5*, 6852–6857. [[CrossRef](#)]
55. Zhang, R.; Liu, Y.; Wang, Z.; Wang, P.; Zheng, Z.; Qin, X.; Zhang, X.; Dai, Y.; Whangbo, M.-H.; Huang, B. Selective photocatalytic conversion of alcohol to aldehydes by singlet oxygen over Bi-based metal-organic frameworks under UV–vis light irradiation. *Appl. Catal. B Environ.* **2019**, *254*, 463–470. [[CrossRef](#)]
56. Li, Q.-Y.; Ma, Z.; Zhang, W.-Q.; Xu, J.-L.; Wei, W.; Lu, H.; Zhao, X.; Wang, X.-J. AIE-active tetraphenylethene functionalized metal–organic framework for selective detection of nitroaromatic explosives and organic photocatalysis. *Chem. Commun.* **2016**, *52*, 11284–11287. [[CrossRef](#)] [[PubMed](#)]
57. Zeng, L.; Liu, T.; He, C.; Shi, D.; Zhang, F.; Duan, C. Organized Aggregation Makes Insoluble Perylene Diimide Efficient for the Reduction of Aryl Halides via Consecutive Visible Light-Induced Electron-Transfer Processes. *J. Am. Chem. Soc.* **2016**, *138*, 3958–3961. [[CrossRef](#)]
58. Zhang, W.-Q.; Li, Q.-Y.; Zhang, Q.; Lu, Y.; Lu, H.; Wang, W.; Zhao, X.; Wang, X.-J. Robust Metal–Organic Framework Containing Benzoselenadiazole for Highly Efficient Aerobic Cross-dehydrogenative Coupling Reactions under Visible Light. *Inorg. Chem.* **2016**, *55*, 1005–1007. [[CrossRef](#)]
59. Wang, C.; Xie, Z.; DeKrafft, K.E.; Lin, W. Doping Metal–Organic Frameworks for Water Oxidation, Carbon Dioxide Reduction, and Organic Photocatalysis. *J. Am. Chem. Soc.* **2011**, *133*, 13445–13454. [[CrossRef](#)]
60. Liu, M.; Guo, L.; Jin, S.; Tan, B. Covalent triazine frameworks: Synthesis and applications. *J. Mater. Chem. A* **2019**, *7*, 5153–5172. [[CrossRef](#)]
61. Krishnaraj, C.; Jena, H.S.; Leus, K.; Van Der Voort, P. Covalent triazine frameworks—A sustainable perspective. *Green Chem.* **2020**, *22*, 1038–1071. [[CrossRef](#)]
62. Jiménez-Almarza, A.; López-Magano, A.; Marzo, L.; Cabrera, S.; Mas-Ballesté, R.; Alemán, J. Imine-Based Covalent Organic Frameworks as Photocatalysts for Metal Free Oxidation Processes under Visible Light Conditions. *ChemCatChem* **2019**, *11*, 4916. [[CrossRef](#)]
63. Chen, R.; Shi, J.-L.; Ma, Y.; Lin, G.; Lang, X.; Wang, C. Designed Synthesis of a 2D Porphyrin-Based sp<sup>2</sup> Carbon-Conjugated Covalent Organic Framework for Heterogeneous Photocatalysis. *Angew. Chem. Int. Ed.* **2019**, *58*, 6430–6434. [[CrossRef](#)]
64. Huang, W.; Ma, B.C.; Lu, H.; Li, R.; Wang, L.; Landfester, K.; Zhang, K.A.I. Visible-Light-Promoted Selective Oxidation of Alcohols Using a Covalent Triazine Framework. *ACS Catal.* **2017**, *7*, 5438–5442. [[CrossRef](#)]
65. Liu, Z.; Su, Q.; Ju, P.; Li, X.; Li, G.; Wu, Q.; Yang, B. A hydrophilic covalent organic framework for photocatalytic oxidation of benzylamine in water. *Chem. Commun.* **2020**, *56*, 766–769. [[CrossRef](#)]
66. Wei, P.-F.; Qi, M.-Z.; Wang, Z.-P.; Ding, S.-Y.; Yu, W.; Liu, Q.; Wang, L.-K.; Wang, H.-Z.; An, W.-K.; Wang, W. Benzoxazole-Linked Ultrastable Covalent Organic Frameworks for Photocatalysis. *J. Am. Chem. Soc.* **2018**, *140*, 4623–4631. [[CrossRef](#)]
67. Kang, X.; Wu, X.; Han, X.; Yuan, C.; Liu, Y.; Cui, Y. Rational synthesis of interpenetrated 3D covalent organic frameworks for asymmetric photocatalysis. *Chem. Sci.* **2020**, *11*, 1494–1502. [[CrossRef](#)]
68. Zhang, R.; Song, X.; Liu, Y.; Wang, P.; Wang, Z.; Zheng, Z.; Dai, Y.; Huang, B. Monomolecular VB<sub>2</sub>-doped MOFs for photocatalytic oxidation with enhanced stability, recyclability and selectivity. *J. Mater. Chem. A* **2019**, *7*, 26934–26943. [[CrossRef](#)]

69. Quan, Y.; Li, Q.-Y.; Zhang, Q.; Zhang, W.-Q.; Lu, H.; Yu, J.-H.; Chen, J.; Zhao, X.; Wang, X.-J. A diiodo-BODIPY postmodified metal–organic framework for efficient heterogeneous organo-photocatalysis. *RSC Adv.* **2016**, *6*, 23995–23999. [[CrossRef](#)]
70. Kumar, G.; Solanki, P.; Nazish, M.; Neogi, S.; Kureshy, R.I.; Khan, N.H. Covalently hooked EOSIN-Y in a Zr(IV) framework as visible-light mediated, heterogeneous photocatalyst for efficient CH functionalization of tertiary amines. *J. Catal.* **2019**, *371*, 298–304. [[CrossRef](#)]
71. Santiago-Portillo, A.; Remiro-Buenamañana, S.; Navalón, S.; García, H. Subphthalocyanine encapsulated within MIL-101(Cr)-NH<sub>2</sub> as a solar light photoredox catalyst for dehalogenation of  $\alpha$ -haloacetophenones. *Dalt. Trans.* **2019**, *48*, 17735–17740. [[CrossRef](#)]
72. López-Magano, A.; Platero-Prats, A.E.; Cabrera, S.; Mas-Ballesté, R.; Alemán, J. Incorporation of Photocatalytic Pt(II) Complexes into Imine-Based Layered Covalent Organic Frameworks (COFs) through Monomer Truncation Strategy. *Appl. Catal. B Environ.* **2020**, *272*, 119027. [[CrossRef](#)]
73. Han, Q.; Wang, Y.-L.; Sun, M.; Sun, C.-Y.; Zhu, S.-S.; Wang, X.-L.; Su, Z.-M. Metal–Organic Frameworks with Organogold(III) Complexes for Photocatalytic Amine Oxidation with Enhanced Efficiency and Selectivity. *Chem.—Eur. J.* **2018**, *24*, 15089–15095. [[CrossRef](#)]
74. Chen, L.; Peng, Y.; Wang, H.; Gu, Z.; Duan, C. Synthesis of Au@ZIF-8 single- or multi-core–shell structures for photocatalysis. *Chem. Commun.* **2014**, *50*, 8651–8654. [[CrossRef](#)] [[PubMed](#)]
75. Fu, Y.; Sun, L.; Yang, H.; Xu, L.; Zhang, F.; Zhu, W. Visible-light-induced aerobic photocatalytic oxidation of aromatic alcohols to aldehydes over Ni-doped NH<sub>2</sub>-MIL-125(Ti). *Appl. Catal. B Environ.* **2016**, *187*, 212–217. [[CrossRef](#)]
76. Wang, T.; Tao, X.; Xiao, Y.; Qiu, G.; Yang, Y.; Li, B. Charge separation and molecule activation promoted by Pd/MIL-125-NH<sub>2</sub> hybrid structures for selective oxidation reactions. *Catal. Sci. Technol.* **2020**, *10*, 138–146. [[CrossRef](#)]
77. Fu, S.-S.; Ren, X.-Y.; Guo, S.; Lan, G.; Zhang, Z.-M.; Lu, T.-B.; Lin, W. Synergistic Effect over Sub-nm Pt Nanocluster@MOFs Significantly Boosts Photo-oxidation of N-alkyl(iso)quinolinium Salts. *iScience* **2020**, *23*, 100793. [[CrossRef](#)] [[PubMed](#)]
78. Wang, D.; Pan, Y.; Xu, L.; Li, Z. PdAu@MIL-100(Fe) cooperatively catalyze tandem reactions between amines and alcohols for efficient N-alkyl amines syntheses under visible light. *J. Catal.* **2018**, *361*, 248–254. [[CrossRef](#)]
79. Sun, D.; Xu, M.; Jiang, Y.; Long, J.; Li, Z. Small-Sized Bimetallic CuPd Nanoclusters Encapsulated Inside Cavity of NH<sub>2</sub>-UiO-66(Zr) with Superior Performance for Light-Induced Suzuki Coupling Reaction. *Small Methods* **2018**, *2*, 1800164. [[CrossRef](#)]
80. Ke, F.; Wang, L.; Zhu, J. Facile fabrication of CdS-metal-organic framework nanocomposites with enhanced visible-light photocatalytic activity for organic transformation. *Nano Res.* **2015**, *8*, 1834–1846. [[CrossRef](#)]
81. Zhang, Q.; Liu, J.-B.; Chen, L.; Xiao, C.-X.; Chen, P.; Shen, S.; Guo, J.-K.; Au, C.-T.; Yin, S.-F. An etching and re-growth method for the synthesis of bismuth ferrite/MIL-53(Fe) nanocomposite as efficient photocatalyst for selective oxidation of aromatic alcohols. *Appl. Catal. B Environ.* **2020**, *264*, 118529. [[CrossRef](#)]
82. Cai, J.; Lu, J.-Y.; Chen, Q.-Y.; Qu, L.-L.; Lu, Y.-Q.; Gao, G.-F. Eu-Based MOF/graphene oxide composite: A novel photocatalyst for the oxidation of benzyl alcohol using water as oxygen source. *New J. Chem.* **2017**, *41*, 3882–3886. [[CrossRef](#)]
83. Zheng, D.-Y.; Chen, E.-X.; Ye, C.-R.; Huang, X.-C. High-efficiency photo-oxidation of thioethers over C60@PCN-222 under air. *J. Mater. Chem. A* **2019**, *7*, 22084–22091. [[CrossRef](#)]
84. Lu, G.; Huang, X.; Li, Y.; Zhao, G.; Pang, G.; Wang, G. Covalently integrated core-shell MOF@COF hybrids as efficient visible-light-driven photocatalysts for selective oxidation of alcohols. *J. Energy Chem.* **2020**, *43*, 8–15. [[CrossRef](#)]
85. Lu, G.; Huang, X.; Wu, Z.; Li, Y.; Xing, L.; Gao, H.; Dong, W.; Wang, G. Construction of covalently integrated core-shell TiO<sub>2</sub> nanobelts@COF hybrids for highly selective oxidation of alcohols under visible light. *Appl. Surf. Sci.* **2019**, *493*, 551–560. [[CrossRef](#)]
86. Long, J.; Wang, S.; Ding, Z.; Wang, S.; Zhou, Y.; Huang, L.; Wang, X. Amine-functionalized zirconium metal–organic framework as efficient visible-light photocatalyst for aerobic organic transformations. *Chem. Commun.* **2012**, *48*, 11656–11658. [[CrossRef](#)]
87. Goh, T.W.; Xiao, C.; Maligal-Ganesh, R.V.; Li, X.; Huang, W. Utilizing mixed-linker zirconium based metal-organic frameworks to enhance the visible light photocatalytic oxidation of alcohol. *Chem. Eng. Sci.* **2015**, *124*, 45–51. [[CrossRef](#)]



88. Chambers, M.B.; Wang, X.; Ellezam, L.; Ersen, O.; Fontecave, M.; Sanchez, C.; Rozes, L.; Mellot-Draznieks, C. Maximizing the Photocatalytic Activity of Metal–Organic Frameworks with Aminated-Functionalized Linkers: Substoichiometric Effects in MIL-125-NH<sub>2</sub>. *J. Am. Chem. Soc.* **2017**, *139*, 8222–8228. [[CrossRef](#)] [[PubMed](#)]
89. Campanelli, M.; Del Giacco, T.; De Angelis, F.; Mosconi, E.; Taddei, M.; Marmottini, F.; D’Amato, R.; Costantino, F. Solvent-Free Synthetic Route for Cerium(IV) Metal–Organic Frameworks with UiO-66 Architecture and Their Photocatalytic Applications. *ACS Appl. Mater. Interfaces* **2019**, *11*, 45031–45037. [[CrossRef](#)]
90. Qiu, X.; Zhu, Y.; Zhang, X.; Zhang, Y.; Menisa, L.T.; Xia, C.; Liu, S.; Tang, Z. Cerium-Based Metal–Organic Frameworks with UiO Architecture for Visible Light-Induced Aerobic Oxidation of Benzyl Alcohol. *Sol. RRL* **2019**. [[CrossRef](#)]
91. Wu, Z.; Huang, X.; Zheng, H.; Wang, P.; Hai, G.; Dong, W.; Wang, G. Aromatic heterocycle-grafted NH<sub>2</sub>-MIL-125(Ti) via conjugated linker with enhanced photocatalytic activity for selective oxidation of alcohols under visible light. *Appl. Catal. B Environ.* **2018**, *224*, 479–487. [[CrossRef](#)]
92. Isaka, Y.; Kondo, Y.; Kuwahara, Y.; Mori, K.; Yamashita, H. Incorporation of a Ru complex into an amine-functionalized metal–organic framework for enhanced activity in photocatalytic aerobic benzyl alcohol oxidation. *Catal. Sci. Technol.* **2019**, *9*, 1511–1517. [[CrossRef](#)]
93. Xiao, L.; Zhang, Q.; Chen, P.; Chen, L.; Ding, F.; Tang, J.; Li, Y.-J.; Au, C.-T.; Yin, S.-F. Copper-mediated metal-organic framework as efficient photocatalyst for the partial oxidation of aromatic alcohols under visible-light irradiation: Synergism of plasmonic effect and schottky junction. *Appl. Catal. B Environ.* **2019**, *248*, 380–387. [[CrossRef](#)]
94. Wojaczyńska, E.; Wojaczyński, J. Enantioselective Synthesis of Sulfoxides: 2000–2009. *Chem. Rev.* **2010**, *110*, 4303–4356. [[CrossRef](#)] [[PubMed](#)]
95. Bonesi, S.M.; Manet, I.; Freccero, M.; Fagnoni, M.; Albini, A. Photosensitized Oxidation of Sulfides: Discriminating between the Singlet-Oxygen Mechanism and Electron Transfer Involving Superoxide Anion or Molecular Oxygen. *Chem.—Eur. J.* **2006**, *12*, 4844–4857. [[CrossRef](#)] [[PubMed](#)]
96. Dad’ová, J.; Svobodová, E.; Sikorski, M.; König, B.; Cibulka, R. Photooxidation of Sulfides to Sulfoxides Mediated by Tetra-O-Acetylruboflavin and Visible Light. *ChemCatChem* **2012**, *4*, 620–623. [[CrossRef](#)]
97. Yan, X.; Liu, H.; Li, Y.; Chen, W.; Zhang, T.; Zhao, Z.; Xing, G.; Chen, L. Ultrastable Covalent Organic Frameworks via Self-Polycondensation of an A<sub>2</sub>B<sub>2</sub> Monomer for Heterogeneous Photocatalysis. *Macromolecules* **2019**, *52*, 7977–7983. [[CrossRef](#)]
98. Meng, Y.; Luo, Y.; Shi, J.-L.; Ding, H.; Lang, X.; Chen, W.; Zheng, A.; Sun, J.; Wang, C. 2D and 3D Porphyrinic Covalent Organic Frameworks: The Influence of Dimensionality on Functionality. *Angew. Chemie Int. Ed.* **2020**, *59*, 3624–3629. [[CrossRef](#)]
99. Liu, L.; Zhang, B.; Tan, X.; Tan, D.; Cheng, X.; Han, B.; Zhang, J. Improved photocatalytic performance of Covalent Organic Frameworks by nanostructure construction. *Chem. Commun.* **2020**, *56*, 4567–4570. [[CrossRef](#)]
100. Zou, Y.-Q.; Chen, J.-R.; Liu, X.-P.; Lu, L.-Q.; Davis, R.L.; Jørgensen, K.A.; Xiao, W.-J. Highly Efficient Aerobic Oxidative Hydroxylation of Arylboronic Acids: Photoredox Catalysis Using Visible Light. *Angew. Chem. Int. Ed.* **2012**, *51*, 784–788. [[CrossRef](#)]
101. Toyao, T.; Ueno, N.; Miyahara, K.; Matsui, Y.; Kim, T.-H.; Horiuchi, Y.; Ikeda, H.; Matsuoka, M. Visible-light, photoredox catalyzed, oxidative hydroxylation of arylboronic acids using a metal–organic framework containing tetrakis(carboxyphenyl)porphyrin groups. *Chem. Commun.* **2015**, *51*, 16103–16106. [[CrossRef](#)]
102. Yu, X.; Cohen, S.M. Photocatalytic metal–organic frameworks for the aerobic oxidation of arylboronic acids. *Chem. Commun.* **2015**, *51*, 9880–9883. [[CrossRef](#)]
103. Funes-Ardoiz, I.; Maseras, F. Oxidative Coupling Mechanisms: Current State of Understanding. *ACS Catal.* **2018**, *8*, 1161–1172. [[CrossRef](#)]
104. Xu, C.; Liu, H.; Li, D.; Su, J.-H.; Jiang, H.-L. Direct evidence of charge separation in a metal–organic framework: Efficient and selective photocatalytic oxidative coupling of amines via charge and energy transfer. *Chem. Sci.* **2018**, *9*, 3152–3158. [[CrossRef](#)] [[PubMed](#)]
105. Liu, R.; Meng, S.; Ma, Y.; Niu, L.; He, S.; Xu, X.; Su, B.; Lu, D.; Yang, Z.; Lei, Z. Atmospheric oxidative coupling of amines by UiO-66-NH<sub>2</sub> photocatalysis under milder reaction conditions. *Catal. Commun.* **2019**, *124*, 108–112. [[CrossRef](#)]

106. Wu, R.; Wang, S.; Zhou, Y.; Long, J.; Dong, F.; Zhang, W. Chromium-Based Metal–Organic Framework MIL-101 Decorated with CdS Quantum Dots for the Photocatalytic Synthesis of Imines. *ACS Appl. Nano Mater.* **2019**, *2*, 6818–6827. [[CrossRef](#)]
107. Luis-Barrerra, J.; Cano, R.; Imani-Shakibaei, G.; Heras-Domingo, J.; Pérez-Carvajal, J.; Imaz, I.; Maspoch, D.; Solans-Monfort, X.; Alemán, J.; Mas-Ballesté, R. Switching acidic and basic catalysis through supramolecular functionalization in a porous 3D covalent imine-based material. *Catal. Sci. Technol.* **2019**, *9*, 6007–6014. [[CrossRef](#)]
108. Bartling, H.; Eisenhofer, A.; König, B.; Gschwind, R.M. The Photocatalyzed Aza-Henry Reaction of N-Aryltetrahydroisoquinolines: Comprehensive Mechanism, H•– versus H+–Abstraction, and Background Reactions. *J. Am. Chem. Soc.* **2016**, *138*, 11860–11871. [[CrossRef](#)] [[PubMed](#)]
109. Liu, J.; Zhang, K.; Chen, Z.; Wei, Z.-W.; Zhang, L. A Porous and Stable Porphyrin Metal–Organic Framework as an Efficient Catalyst towards Visible-Light-Mediated Aerobic Cross-Dehydrogenative-Coupling Reactions. *Chem.—Asian J.* **2020**, *15*, 1118. [[CrossRef](#)]
110. Zhi, Y.; Li, Z.; Feng, X.; Xia, H.; Zhang, Y.; Shi, Z.; Mu, Y.; Liu, X. Covalent organic frameworks as metal-free heterogeneous photocatalysts for organic transformations. *J. Mater. Chem. A* **2017**, *5*, 22933–22938. [[CrossRef](#)]
111. Wild, S.; McLagan, D.; Schlabach, M.; Bossi, R.; Hawker, D.; Cropp, R.; King, C.K.; Stark, J.S.; Mondon, J.; Nash, S.B. An Antarctic Research Station as a Source of Brominated and Perfluorinated Persistent Organic Pollutants to the Local Environment. *Environ. Sci. Technol.* **2015**, *49*, 103–112. [[CrossRef](#)]
112. Yin, H.; Wada, Y.; Kitamura, T.; Yanagida, S. Photoreductive Dehalogenation of Halogenated Benzene Derivatives Using ZnS or CdS Nanocrystallites as Photocatalysts. *Environ. Sci. Technol.* **2001**, *35*, 227–231. [[CrossRef](#)]
113. Shih, H.-W.; Vander Wal, M.N.; Grange, R.L.; MacMillan, D.W.C. Enantioselective  $\alpha$ -Benzoylation of Aldehydes via Photoredox Organocatalysis. *J. Am. Chem. Soc.* **2010**, *132*, 13600–13603. [[CrossRef](#)]
114. Wu, P.; He, C.; Wang, J.; Peng, X.; Li, X.; An, Y.; Duan, C. Photoactive Chiral Metal–Organic Frameworks for Light-Driven Asymmetric  $\alpha$ -Alkylation of Aldehydes. *J. Am. Chem. Soc.* **2012**, *134*, 14991–14999. [[CrossRef](#)] [[PubMed](#)]
115. Santiago-Portillo, A.; Baldoví, H.G.; Carbonell, E.; Navalón, S.; Álvaro, M.; García, H.; Ferrer, B. Ruthenium(II) Tris(2,2'-bipyridyl) Complex Incorporated in UiO-67 as Photoredox Catalyst. *J. Phys. Chem. C* **2018**, *122*, 29190–29199. [[CrossRef](#)]
116. Peng, W.; Lin, Y.; Wan, Z.; Ji, H.; Ma, W.; Zhao, J. An unusual dependency on the hole-scavengers in photocatalytic reductions mediated by a titanium-based metal-organic framework. *Catal. Today* **2020**, *340*, 86–91. [[CrossRef](#)]
117. Li, Z.; Zhi, Y.; Shao, P.; Xia, H.; Li, G.; Feng, X.; Chen, X.; Shi, Z.; Liu, X. Covalent organic framework as an efficient, metal-free, heterogeneous photocatalyst for organic transformations under visible light. *Appl. Catal. B Environ.* **2019**, *245*, 334–342. [[CrossRef](#)]
118. Yu, X.; Cohen, S.M. Photocatalytic Metal–Organic Frameworks for Selective 2,2,2-Trifluoroethylation of Styrenes. *J. Am. Chem. Soc.* **2016**, *138*, 12320–12323. [[CrossRef](#)] [[PubMed](#)]
119. Azarifar, D.; Ghorbani-Vaghei, R.; Daliran, S.; Oveisi, A.R. A Multifunctional Zirconium-Based Metal–Organic Framework for the One-Pot Tandem Photooxidative Passerini Three-Component Reaction of Alcohols. *ChemCatChem* **2017**, *9*, 1992–2000. [[CrossRef](#)]
120. Huang, W.; Wang, Z.J.; Ma, B.C.; Ghasimi, S.; Gehrig, D.; Laquai, F.; Landfester, K.; Zhang, K.A.I. Hollow nanoporous covalent triazine frameworks via acid vapor-assisted solid phase synthesis for enhanced visible light photoactivity. *J. Mater. Chem. A* **2016**, *4*, 7555–7559. [[CrossRef](#)]
121. Huang, W.; Byun, J.; Rörich, I.; Ramanan, C.; Blom, P.W.M.; Lu, H.; Wang, D.; Caire da Silva, L.; Li, R.; Wang, L.; et al. Asymmetric Covalent Triazine Framework for Enhanced Visible-Light Photoredox Catalysis via Energy Transfer Cascade. *Angew. Chem. Int. Ed.* **2018**, *57*, 8316–8320. [[CrossRef](#)]
122. Liu, S.; Pan, W.; Wu, S.; Bu, X.; Xin, S.; Yu, J.; Xu, H.; Yang, X. Visible-light-induced tandem radical addition–cyclization of 2-aryl phenyl isocyanides catalysed by recyclable covalent organic frameworks. *Green Chem.* **2019**, *21*, 2905–2910. [[CrossRef](#)]
123. Tian, M.; Liu, S.; Bu, X.; Yu, J.; Yang, X. Covalent Organic Frameworks: A Sustainable Photocatalyst toward Visible-Light-Accelerated C3 Arylation and Alkylation of Quinoxalin-2(1H)-ones. *Chem.—Eur. J.* **2020**, *26*, 369–373. [[CrossRef](#)]



124. Yuan, J.; Xia, Q.; Zhu, W.; Wu, C.; Wang, B.; Liu, B.; Yang, X.; Xu, Y.; Xu, H. Sunlight-Driven Synthesis of 1,2,4-Thiadiazoles via Oxidative Construction of a Nitrogen-Sulfur Bond Catalyzed by a Reusable Covalent Organic Framework. *ChemPhotoChem* **2020**. [[CrossRef](#)]
125. Pachfule, P.; Acharjya, A.; Roeser, J.; Sivasankaran, R.P.; Ye, M.-Y.; Brückner, A.; Schmidt, J.; Thomas, A. Donor–acceptor covalent organic frameworks for visible light induced free radical polymerization. *Chem. Sci.* **2019**, *10*, 8316–8322. [[CrossRef](#)] [[PubMed](#)]
126. Sun, D.; Jang, S.; Yim, S.-J.; Ye, L.; Kim, D.-P. Metal Doped Core–Shell Metal–Organic Frameworks@Covalent Organic Frameworks (MOFs@COFs) Hybrids as a Novel Photocatalytic Platform. *Adv. Funct. Mater.* **2018**, *28*, 1707110. [[CrossRef](#)]
127. Zhu, B.; Zou, R.; Xu, Q. Metal–Organic Framework Based Catalysts for Hydrogen Evolution. *Adv. Energy Mater.* **2018**, *8*, 1801193. [[CrossRef](#)]
128. Kidanemariam, A.; Lee, J.; Park, J. Recent Innovation of Metal–Organic Frameworks for Carbon Dioxide Photocatalytic Reduction. *Polymers* **2019**, *11*, 2090. [[CrossRef](#)]
129. Lorén, N.; Hagman, J.; Jonasson, J.K.; Deschout, H.; Bernin, D.; Cella-Zanacchi, F.; Diaspro, A.; McNally, J.G.; Ameloot, M.; Smisdom, N.; et al. Fluorescence recovery after photobleaching in material and life sciences: Putting theory into practice. *Q. Rev. Biophys.* **2015**, *48*, 323–387. [[CrossRef](#)]
130. Ding, M.; Cai, X.; Jiang, H.-L. Improving MOF stability: Approaches and applications. *Chem. Sci.* **2019**, *10*, 10209–10230. [[CrossRef](#)]



© 2020 by the authors. Licensee MDPI, Basel, Switzerland. This article is an open access article distributed under the terms and conditions of the Creative Commons Attribution (CC BY) license (<http://creativecommons.org/licenses/by/4.0/>).